自己回帰モデルを用いた重力波データ解析(2)：LIGO/Virgo O2までのカタログデータ解析

ブラックホールリングダウン波形の

真貝寿明（大阪工大）

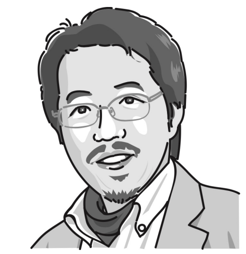

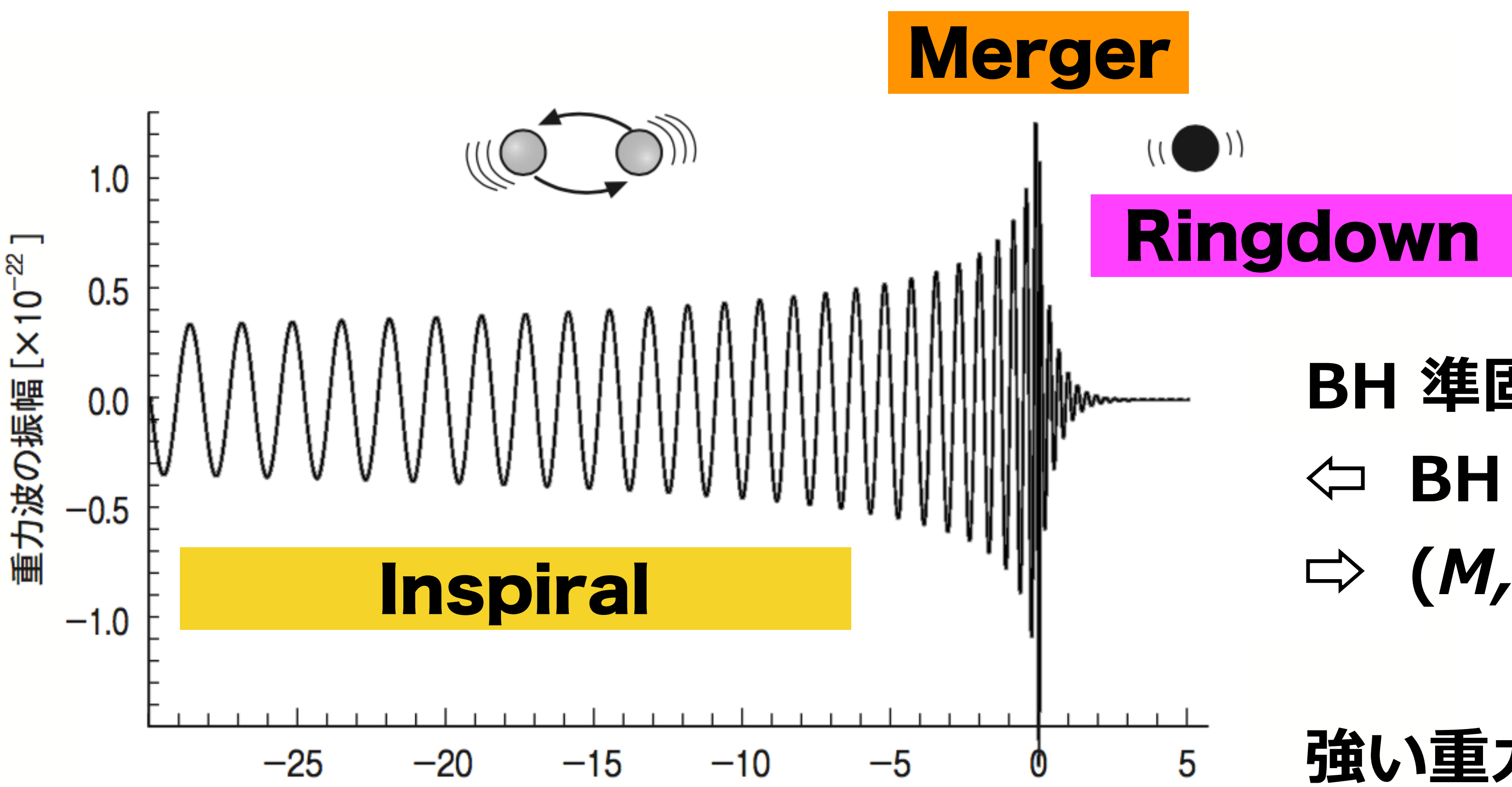

BH 準固有モード(quasi-normal modes)

⇦ BH 摂動理論

⇨ (M, a)

強い重力場の表れ

⇨ 一般相対論の検証ができる

テンプレートを使わず，データから波形を再構築.

2019/9/20 物理学会 @ 山形大学

O1/O2 カタログ

PHYSICAL REVIEW X **9**, 031040 (2019)

GWTC-1: A Gravitational-Wave Transient Catalog of Compact Binary Mergers Observed by LIGO and Virgo during the First and Second Observing Runs

B. P. Abbott *et al.*[*]
(LIGO Scientific Collaboration and Virgo Collaboration)

(Received 14 December 2018; revised manuscript received 27 March 2019; published 4 September 2019)

O1: September 12, 2015 -- January 19, 2016

▶ GW150914 BHBH

O2: November 30, 2016 -- August 25, 2017

▶ GW170817 NSNS

▶ **GWTC-1 catalogue paper [arXiv:1811.12907]**

▶ **data released to public Feb, 2019**

O3a: April 1, 2019 -- September 30, 2019

▶ data released to public April, 2021

O3b: November 1, 2019 -- May 1, 2020

GWTC-1: A GRAVITATIONAL-WAVE TRANSIENT CATALOG ... PHYS. REV. X **9**, 031040 (2019)

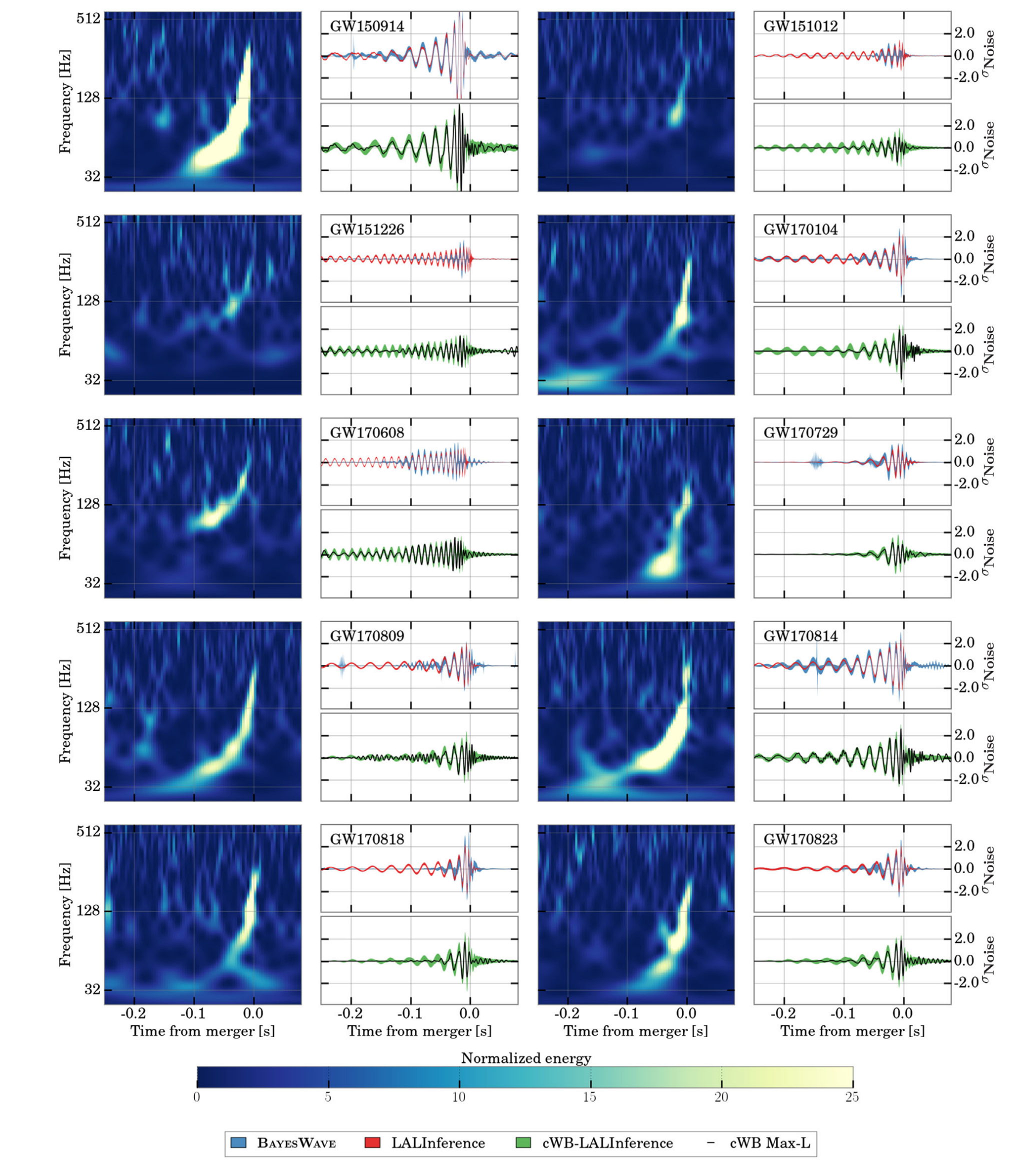

FIG. 10. Time-frequency maps and reconstructed signal waveforms for the ten BBH events. Each event is represented with three panels showing whitened data from the LIGO detector where the higher SNR is recorded. The first panel shows a normalized time-frequency power map of the GW strain. The remaining pair of panels shows time-domain reconstructions of the whitened signal, in units of the standard deviation of the noise. The upper panels show the 90% credible intervals from the posterior probability density functions of the waveform time series, inferred using CBC waveform templates from Bayesian inference (LALInference) with the PhenomP model (red band) and by the BayesWave wavelet model (blue band) [53]. The lower panels show the point estimates from the cWB search (solid lines), along with a 90% confidence interval (green band) derived from cWB analyses of simulated waveforms from the LALInference CBC parameter estimation injected into data near each event. Visible differences between the different reconstruction methods are verified to be consistent with a noise origin (see the text for details).

031040-21

O1/O2 カタログ

Event	$m_1/M_\odot$	$m_2/M_\odot$	$\mathcal{M}/M_\odot$	$\chi_{\rm eff}$	$M_f/M_\odot$	a_f	$E_{\rm rad}/(M_\odot c^2)$	$\ell_{\rm peak}/({\rm erg\,s}^{-1})$	d_L/Mpc	z	$\Delta\Omega/{\rm deg}^2$
GW150914	$35.6^{+4.7}_{-3.1}$	$30.6^{+3.0}_{-4.4}$	$28.6^{+1.7}_{-1.5}$	$-0.01^{+0.12}_{-0.13}$	$63.1^{+3.4}_{-3.0}$	$0.69^{+0.05}_{-0.04}$	$3.1^{+0.4}_{-0.4}$	$3.6^{+0.4}_{-0.4}\times10^{56}$	440^{+150}_{-170}	$0.09^{+0.03}_{-0.03}$	182
GW151012	$23.2^{+14.9}_{-5.5}$	$13.6^{+4.1}_{-4.8}$	$15.2^{+2.1}_{-1.2}$	$0.05^{+0.31}_{-0.20}$	$35.6^{+10.8}_{-3.8}$	$0.67^{+0.13}_{-0.11}$	$1.6^{+0.6}_{-0.5}$	$3.2^{+0.8}_{-1.7}\times10^{56}$	1080^{+550}_{-490}	$0.21^{+0.09}_{-0.09}$	1523
GW151226	$13.7^{+8.8}_{-3.2}$	$7.7^{+2.2}_{-2.5}$	$8.9^{+0.3}_{-0.3}$	$0.18^{+0.20}_{-0.12}$	$20.5^{+6.4}_{-1.5}$	$0.74^{+0.07}_{-0.05}$	$1.0^{+0.1}_{-0.2}$	$3.4^{+0.7}_{-1.7}\times10^{56}$	450^{+180}_{-190}	$0.09^{+0.04}_{-0.04}$	1033
GW170104	$30.8^{+7.3}_{-5.6}$	$20.0^{+4.9}_{-4.6}$	$21.4^{+2.2}_{-1.8}$	$-0.04^{+0.17}_{-0.21}$	$48.9^{+5.1}_{-4.0}$	$0.66^{+0.08}_{-0.11}$	$2.2^{+0.5}_{-0.5}$	$3.3^{+0.6}_{-1.0}\times10^{56}$	990^{+440}_{-430}	$0.20^{+0.08}_{-0.08}$	921
GW170608	$11.0^{+5.5}_{-1.7}$	$7.6^{+1.4}_{-2.2}$	$7.9^{+0.2}_{-0.2}$	$0.03^{+0.19}_{-0.07}$	$17.8^{+3.4}_{-0.7}$	$0.69^{+0.04}_{-0.04}$	$0.9^{+0.0}_{-0.1}$	$3.5^{+0.4}_{-1.3}\times10^{56}$	320^{+120}_{-110}	$0.07^{+0.02}_{-0.02}$	392
GW170729	$50.2^{+16.2}_{-10.2}$	$34.0^{+9.1}_{-10.1}$	$35.4^{+6.5}_{-4.8}$	$0.37^{+0.21}_{-0.25}$	$79.5^{+14.7}_{-10.2}$	$0.81^{+0.07}_{-0.13}$	$4.8^{+1.7}_{-1.7}$	$4.2^{+0.9}_{-1.5}\times10^{56}$	2840^{+1400}_{-1360}	$0.49^{+0.19}_{-0.21}$	1041
GW170809	$35.0^{+8.3}_{-5.9}$	$23.8^{+5.1}_{-5.2}$	$24.9^{+2.1}_{-1.7}$	$0.08^{+0.17}_{-0.17}$	$56.3^{+5.2}_{-3.8}$	$0.70^{+0.08}_{-0.09}$	$2.7^{+0.6}_{-0.6}$	$3.5^{+0.6}_{-0.9}\times10^{56}$	1030^{+320}_{-390}	$0.20^{+0.05}_{-0.07}$	308
GW170814	$30.6^{+5.6}_{-3.0}$	$25.2^{+2.8}_{-4.0}$	$24.1^{+1.4}_{-1.1}$	$0.07^{+0.12}_{-0.12}$	$53.2^{+3.2}_{-2.4}$	$0.72^{+0.07}_{-0.05}$	$2.7^{+0.4}_{-0.3}$	$3.7^{+0.4}_{-0.5}\times10^{56}$	600^{+150}_{-220}	$0.12^{+0.03}_{-0.04}$	87
GW170817	$1.46^{+0.12}_{-0.10}$	$1.27^{+0.09}_{-0.09}$	$1.186^{+0.001}_{-0.001}$	$0.00^{+0.02}_{-0.01}$	≤ 2.8	≤ 0.89	≥ 0.04	$\ge 0.1\times10^{56}$	40^{+7}_{-15}	$0.01^{+0.00}_{-0.00}$	16
GW170818	$35.4^{+7.5}_{-4.7}$	$26.7^{+4.3}_{-5.2}$	$26.5^{+2.1}_{-1.7}$	$-0.09^{+0.18}_{-0.21}$	$59.4^{+4.9}_{-3.8}$	$0.67^{+0.07}_{-0.08}$	$2.7^{+0.5}_{-0.5}$	$3.4^{+0.5}_{-0.7}\times10^{56}$	1060^{+420}_{-380}	$0.21^{+0.07}_{-0.07}$	39[illegible]
GW170823	$39.5^{+11.2}_{-6.7}$	$29.0^{+6.7}_{-7.8}$	$29.2^{+4.6}_{-3.6}$	$0.09^{+0.22}_{-0.26}$	$65.4^{+10.1}_{-7.4}$	$0.72^{+0.09}_{-0.12}$	$3.3^{+1.0}_{-0.9}$	$3.6^{+0.7}_{-1.1}\times10^{56}$	1940^{+970}_{-900}	$0.35^{+0.15}_{-0.15}$	1666

TABLE V. KL divergences (in bits) between the prior and posterior for the effective aligned spin $\chi_{\rm eff}$ and the effective precession spin χ_p. For the computation of the KL divergence for χ_p, we quote the KL divergence with the prior conditioned on the $\chi_{\rm eff}$ posterior, $D_{\rm KL}^{\chi_p}(\chi_{\rm eff})$, and without conditioning, $D_{\rm KL}^{\chi_p}$. For GW170817, $D_{\rm KL}^{\chi_p}$ is given for the high spin prior. The median and 90% interval for the KL divergences is estimated by computing the statistic for repeated draws of a subset of the posterior and prior PDFs. Single-detector optimal SNRs from parameter-estimation analyses for Hanford (H), Livingston (L), and Virgo (V).

Event	GW150914	GW151012	GW151226	GW170104	GW170608	GW170729	GW170809	GW170814	GW170817	GW170818	GW170823
$D_{\rm KL}^{\chi_{\rm eff}}$	$0.71^{+0.04}_{-0.03}$	$0.23^{+0.03}_{-0.02}$	$1.32^{+0.11}_{-0.06}$	$0.54^{+0.03}_{-0.03}$	$0.97^{+0.03}_{-0.05}$	$1.83^{+0.07}_{-0.09}$	$0.71^{+0.03}_{-0.03}$	$0.99^{+0.05}_{-0.07}$	$2.32^{+0.08}_{-0.10}$	$0.50^{+0.04}_{-0.03}$	$0.32^{+0.04}_{-0.03}$
$D_{\rm KL}^{\chi_p}$	$0.16^{+0.03}_{-0.02}$	$0.09^{+0.03}_{-0.02}$	$0.17^{+0.03}_{-0.04}$	$0.05^{+0.01}_{-0.01}$	$0.07^{+0.01}_{-0.02}$	$0.09^{+0.02}_{-0.02}$	$0.05^{+0.01}_{-0.01}$	$0.02^{+0.01}_{-0.01}$	$0.19^{+0.04}_{-0.03}$	$0.06^{+0.02}_{-0.01}$	$0.03^{+0.01}_{-0.01}$
$D_{\rm KL}^{\chi_p}(\chi_{\rm eff})$	$0.09^{+0.02}$	$0.08^{+0.02}$	$0.12^{+0.05}$	$0.07^{+0.02}$	$0.08^{+0.02}$	$0.03^{+0.01}$	$0.06^{+0.01}$	$0.13^{+0.03}$	$0.07^{+0.01}$	$0.09^{+0.02}$	$0.03^{+0.01}$
H SNR	$20.6^{+1.6}_{-1.6}$	$6.4^{+1.3}_{-1.3}$	$9.8^{+1.5}_{-1.4}$	$9.5^{+1.3}_{-1.6}$	$12.1^{+1.6}_{-1.6}$	$5.9^{+1.1}_{-1.1}$	$5.9^{+1.4}_{-1.4}$	$9.3^{+1.0}_{-1.2}$	$18.9^{+1.0}_{-1.0}$	$4.6^{+0.9}_{-0.8}$	$6.8^{+1.4}_{-1.2}$
L SNR	$14.2^{+1.6}_{-1.4}$	$5.8^{+1.2}_{-1.2}$	$6.9^{+1.2}_{-1.1}$	$9.9^{+1.5}_{-1.3}$	$9.2^{+1.5}_{-1.2}$	$8.3^{+1.4}_{-1.4}$	$10.7^{+1.6}_{-1.8}$	$14.3^{+1.5}_{-1.4}$	$26.3^{+1.4}_{-1.3}$	$9.7^{+1.5}_{-1.5}$	$9.2^{+1.7}_{-1.5}$
V SNR	...	...	...	...	...	$1.7^{+1.0}_{-1.1}$	$1.1^{+1.2}_{-0.8}$	$4.1^{+1.1}_{-1.1}$	$3.0^{+0.2}_{-0.2}$	$4.2^{+0.8}_{-0.7}$	...

Ring-down modeを独立に見つける手法の比較 (mockdata challenge)

PHYSICAL REVIEW D **99,** 124032 (2019)

Comparison of various methods to extract ringdown frequency from gravitational wave data

Hiroyuki Nakano,[1,*] Tatsuya Narikawa,[2,3,†] Ken-ichi Oohara,[4,‡] Kazuki Sakai,[5,§] Hisa-aki Shinkai,[6,∥] Hirotaka Takahashi,[7,8,¶] Takahiro Tanaka,[3,9,**] Nami Uchikata,[2,4,††] Shun Yamamoto,[6] and Takahiro S. Yamamoto[3,‡‡]

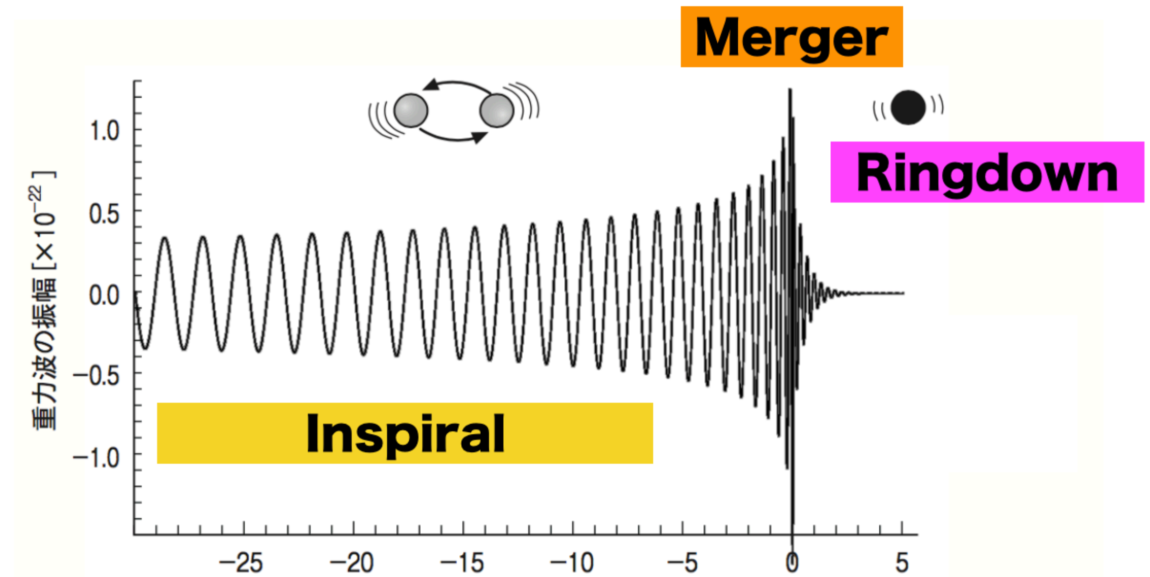

ringdown search
60 mockdata

matched filtering

Hilbert-Huan Transformation

Auto-Regression Method

Neural Network method

TABLE III. We show the values of $\overline{\delta \log f_R}$, $\sigma(f_R)$, $\overline{\delta \log f_I}$, and $\sigma(f_I)$ for various methods. The results limited to set A are given on the first law of each method, while those limited to set B are on the second.

		$\overline{\delta \log f_R}$(%)	$\sigma(f_R)$(%)	$\overline{\delta \log f_I}$(%)	$\sigma(f_I)$(%)
MF-R	A	−12.88	28.36	−71.51	97.79
	B	−0.82	27.53	−46.11	75.48
MF-MR	A	6.25 Very good	17.27 Good	−12.62 Very good	37.9 Very good
	B	2.47	10.41	7.18	27.61
HHT	A	−13.38	21.91	−44.11	61.58
	B	−8.08	19.81	−28.78	49.61
AR	A	0.2 Excellent	9.93 Excellent	4.88 Excellent	38.75 Good
	B	1.91	8.57	6.2	34.64
NN	A	−6.64 Good	16.48 Very good	−15.23 Good	33.96 Excellent
	B	−6.65	11.97	9.96	23.76

1. Auto-Regressive model (Method, general) I

Fitting data with linear func.

$$
\begin{aligned}
x_n &= a_1 x_{n-1} + a_2 x_{n-2} + \cdots + a_M x_{n-M} + \varepsilon \\
&= \sum_{j=1}^{M} a_j x_{n-j} + \varepsilon
\end{aligned}
$$

e.g. $x_n = A e^{-rn\Delta t} \cos(\omega n \Delta t)$

$$Z_1 = e^{-(r-j\omega)\Delta t}$$
$$Z_2 = e^{-(r+j\omega)\Delta t}$$

$$\rightarrow \quad x_n = \frac{A}{2}(Z_1^n + Z_2^n) = (Z_1 + Z_2)x_{n-1} - Z_1 Z_2 x_{n-2}$$

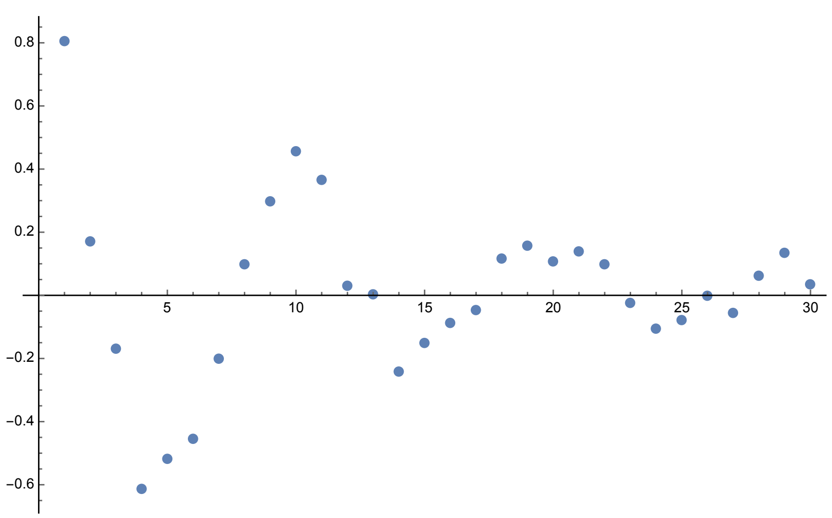

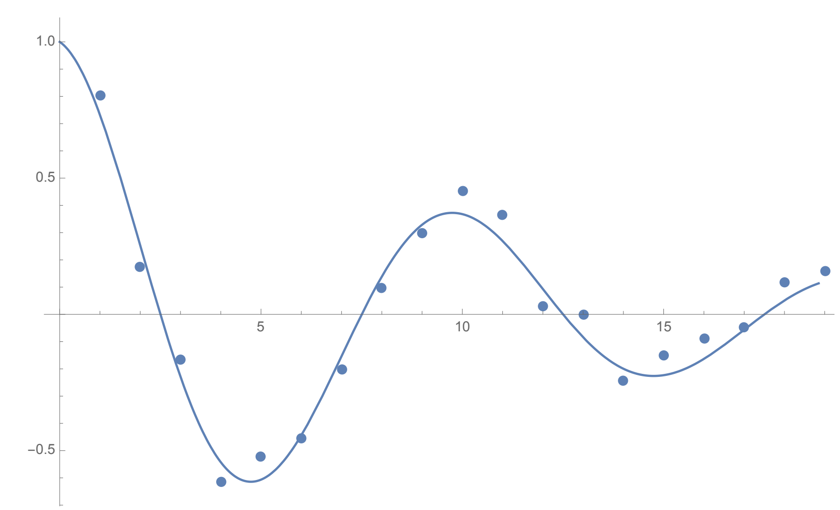

can be applied also to noisy data by adjusting *M*

1. Auto-Regressive model (Method, general) II

Fitting data with linear func.

$$\begin{aligned} x_n &= a_1 x_{n-1} + a_2 x_{n-2} + \cdots + a_M x_{n-M} + \varepsilon \\ &= \sum_{j=1}^{M} a_j x_{n-j} + \varepsilon \end{aligned}$$

- find a_j (Burg method)
- find M (FPE final prediction error method)
- re-construct wave signal from fitted function
- apply FFT with arbitrary precision.

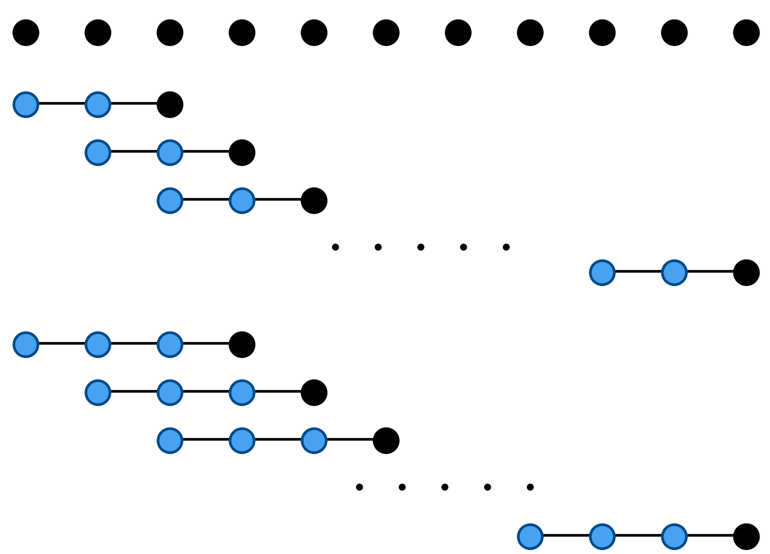

power spectrum

$$p(f) = \frac{\sigma^2}{\left| 1 - \sum_{j=1}^{M} a_j e^{-I 2\pi j f \Delta t} \right|^2}$$

Auto-Regressive model vs Short FFT

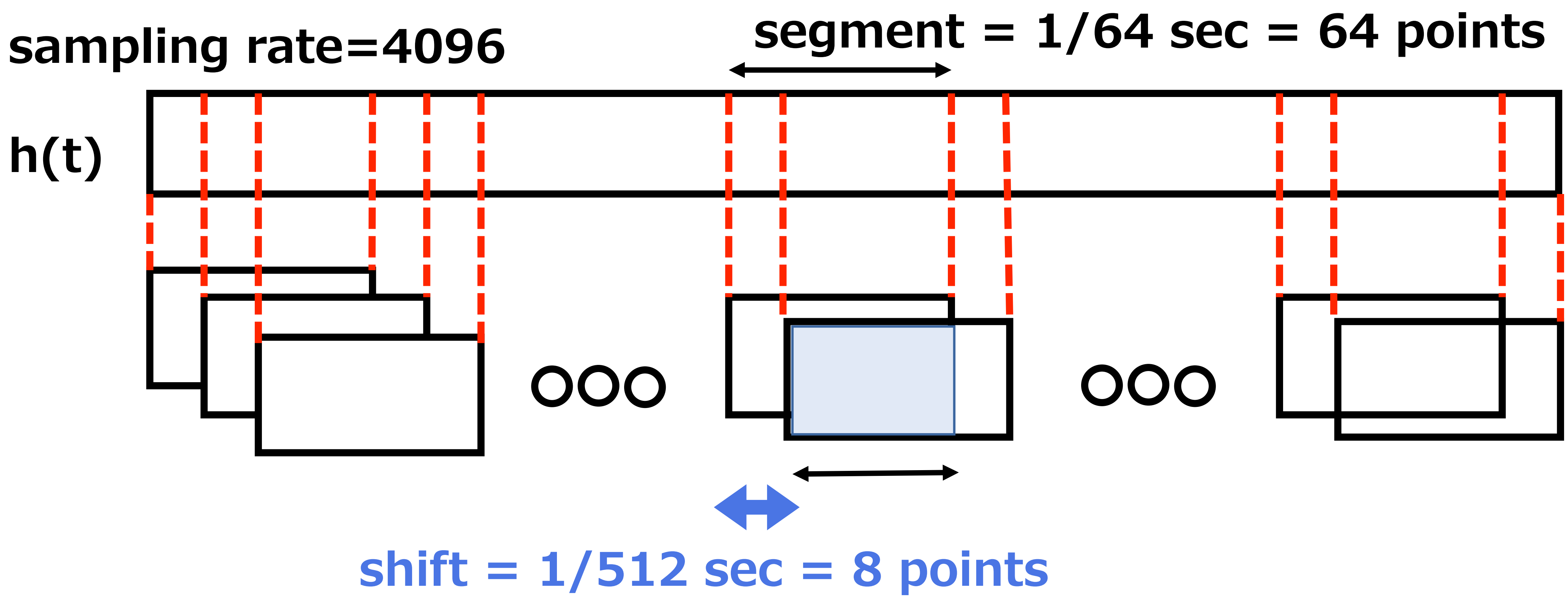

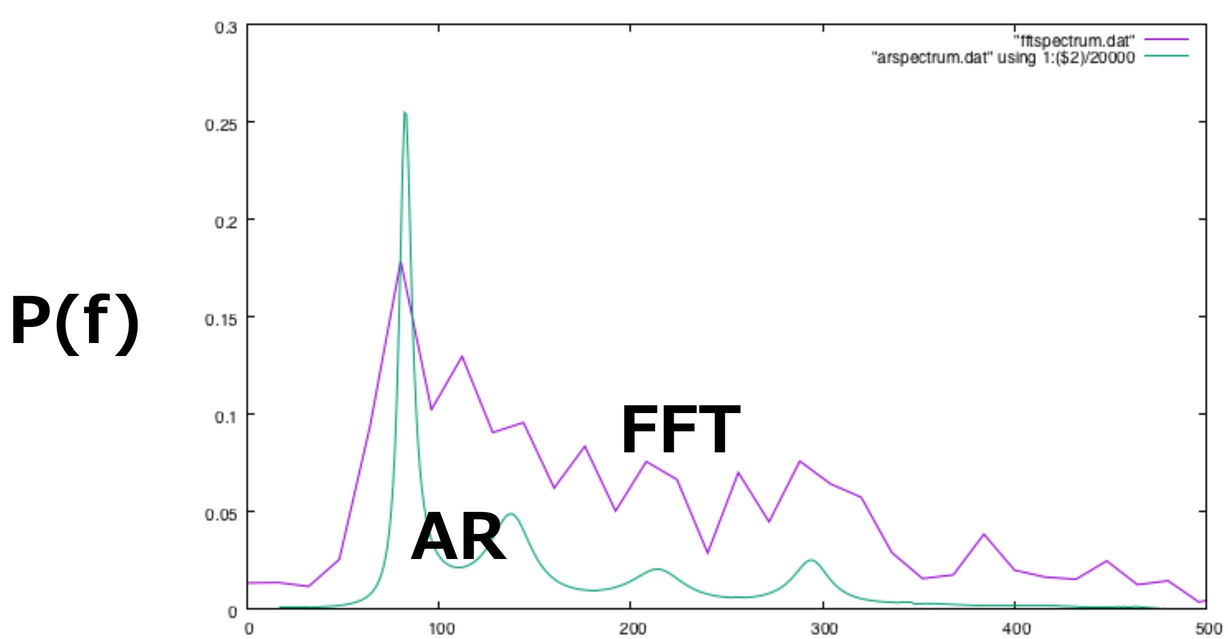

The order *M* can be fixed at 2～8.

Even for short segment, AR model shows precise power-spectrum.

freq. [mock data, SNR=40, inspiral part]

1. Auto-Regressive model (Method, general) III

Fitting data with linear func.

$$
\begin{aligned}
x_n &= a_1 x_{n-1} + a_2 x_{n-2} + \cdots + a_M x_{n-M} + \varepsilon \\
&= \sum_{j=1}^{M} a_j x_{n-j} + \varepsilon
\end{aligned}
$$

- find a_j (Burg method)
- find M (FPE final prediction error method)
- re-construct wave signal from fitted function
- apply FFT with arbitrary precision.

power spectrum

$$
p(f) = \frac{\sigma^2}{\left| 1 - \sum_{j=1}^{M} a_j e^{-I 2\pi j f \Delta t} \right|^2}
$$

characteristic eq.

$$
f(z) = 1 - \sum_{j=1}^{M} a_j z^j = 0
$$

$|z_k|$ says amplitude,
$\arg(z_k)$ says frequency.

GW150914

LIGO paper

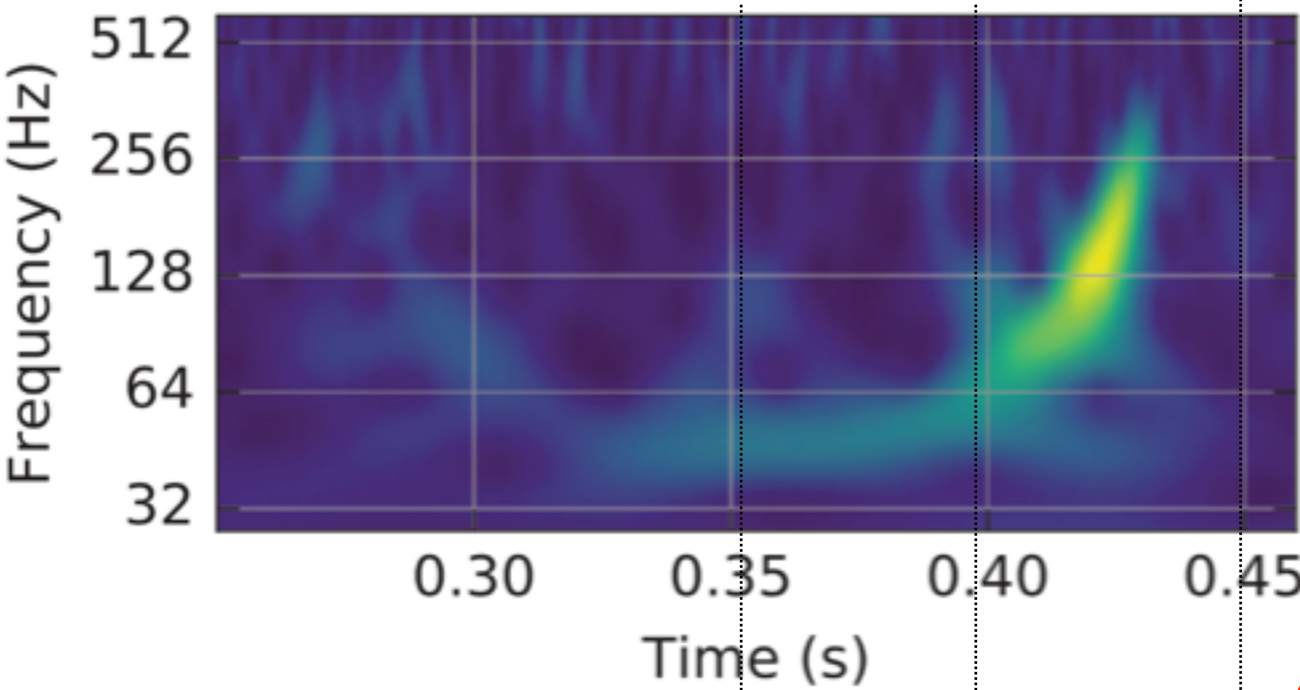

freq [Hz]

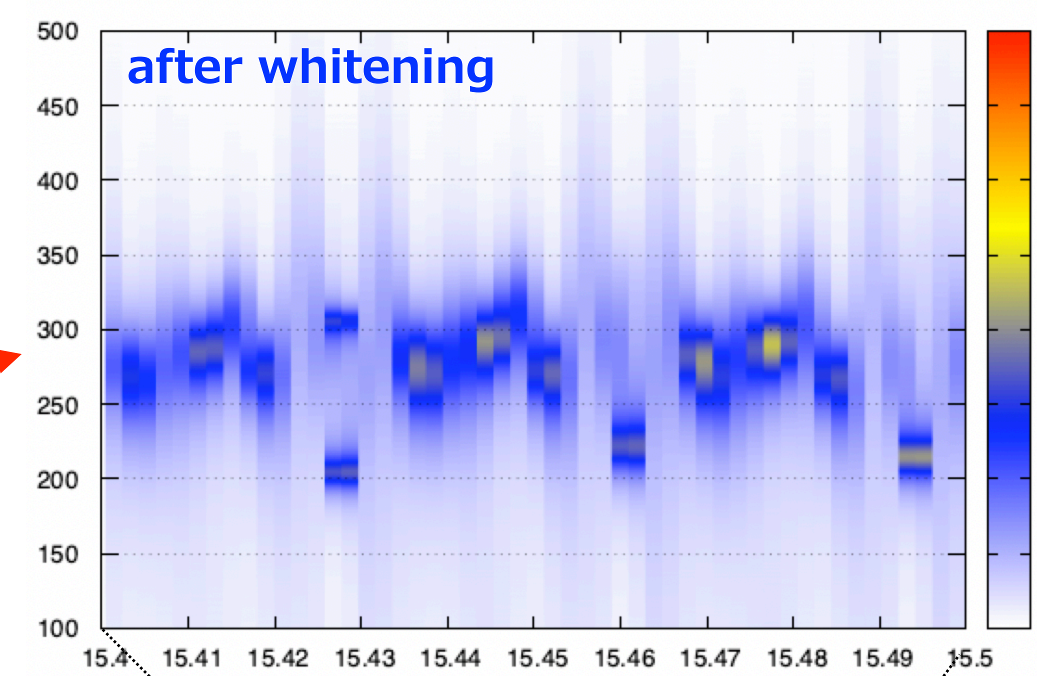

▲merger time

before whitening

AR model Hanford

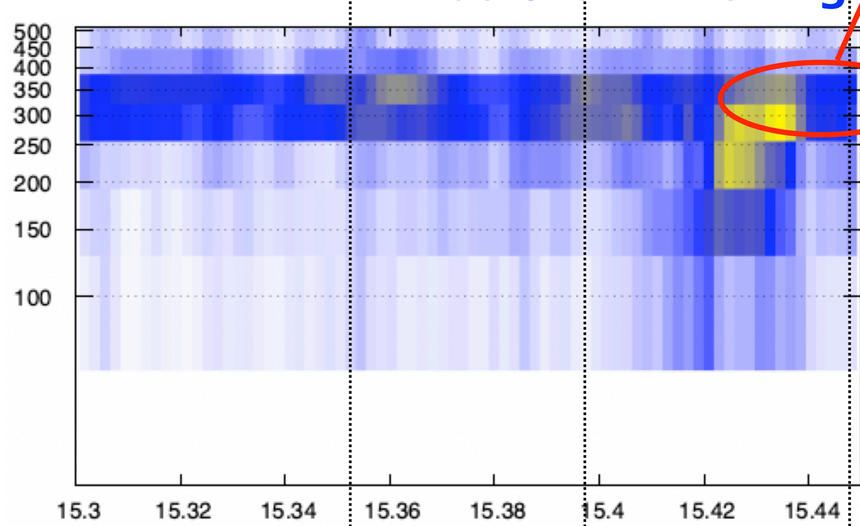

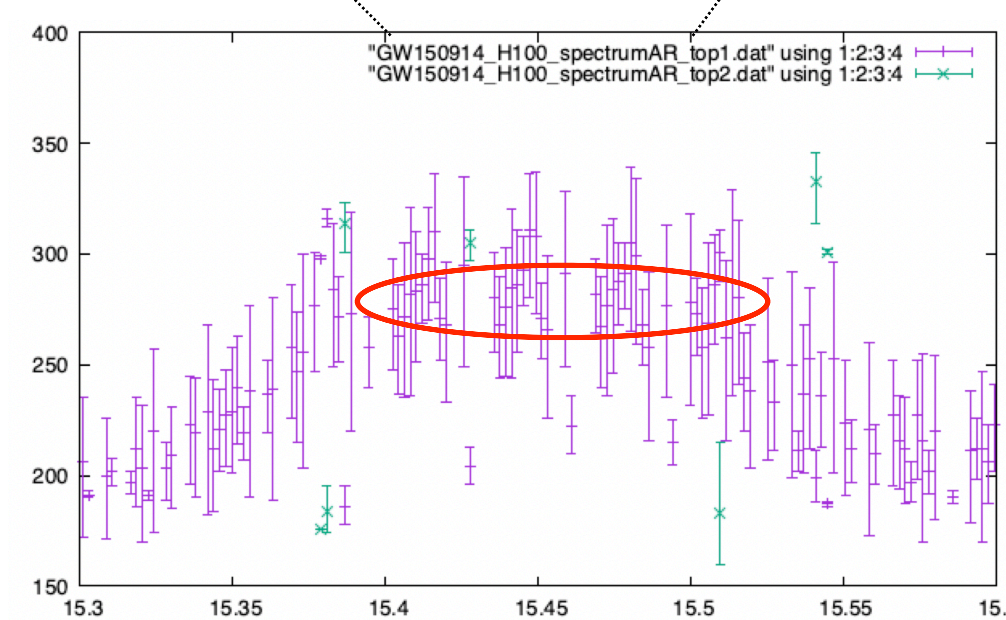

4096 sampling rate
150-450 Hz filter
1 segment = 1/64 sec= 64 points
1 shift = 1/512 sec = 8 points

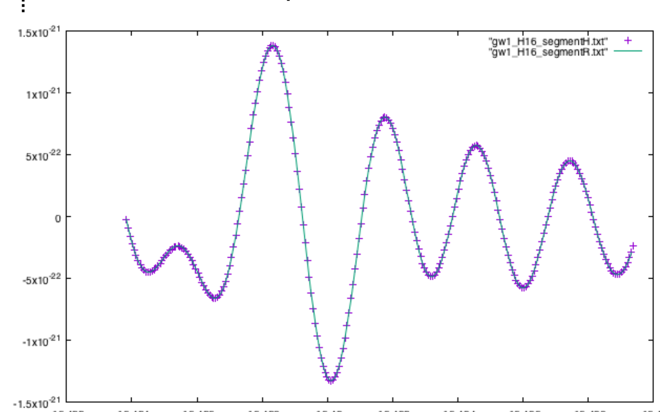

GW150914

Hanford (SNR=20.6)

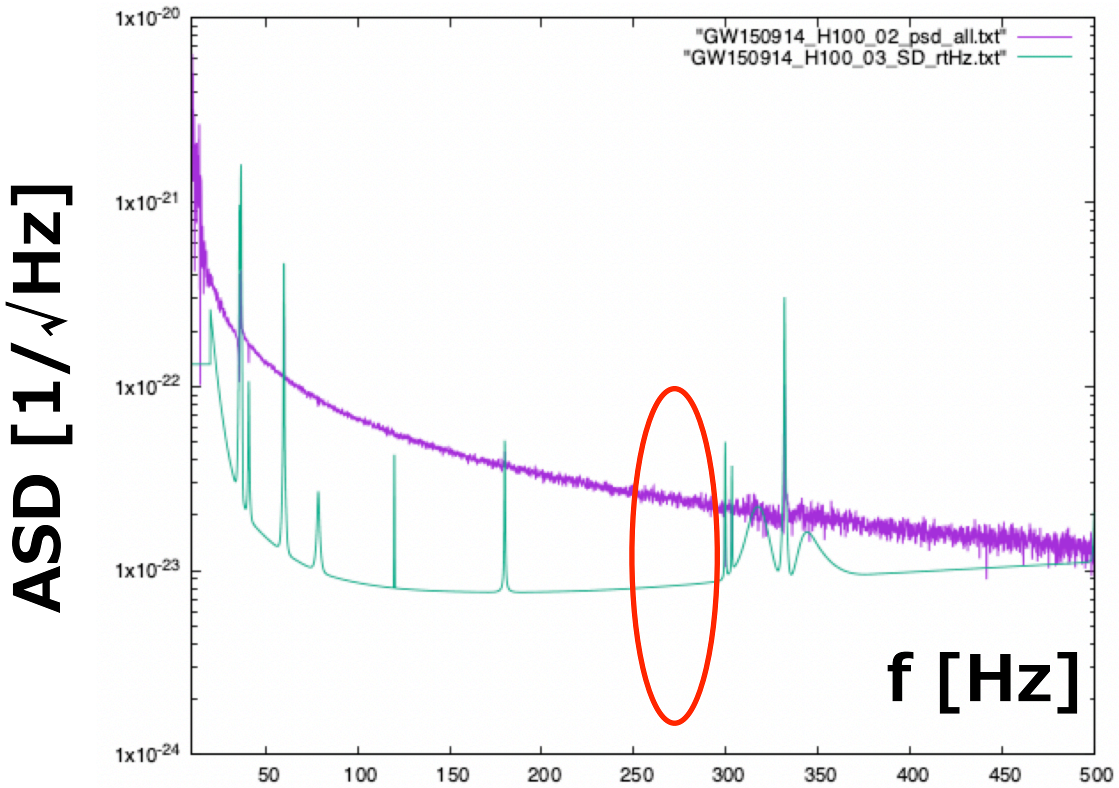

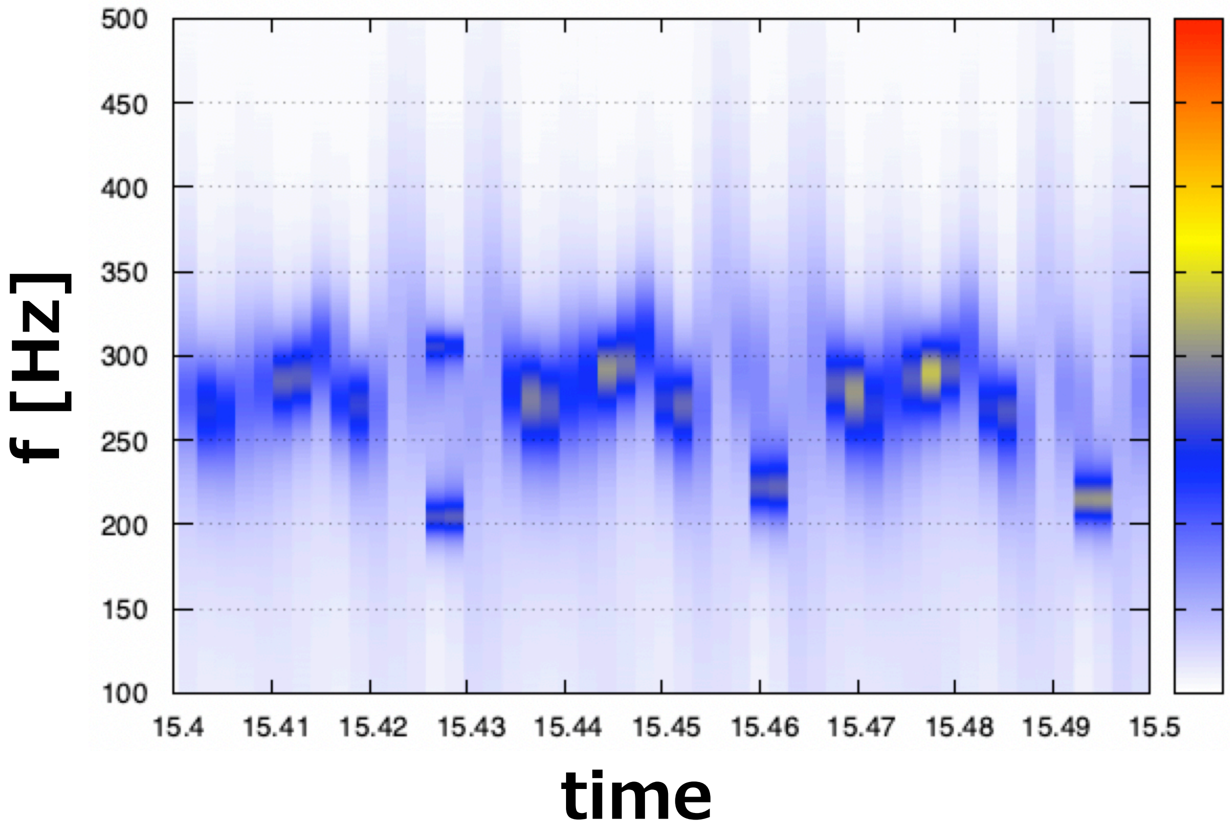

Livingston (SNR=14.2)

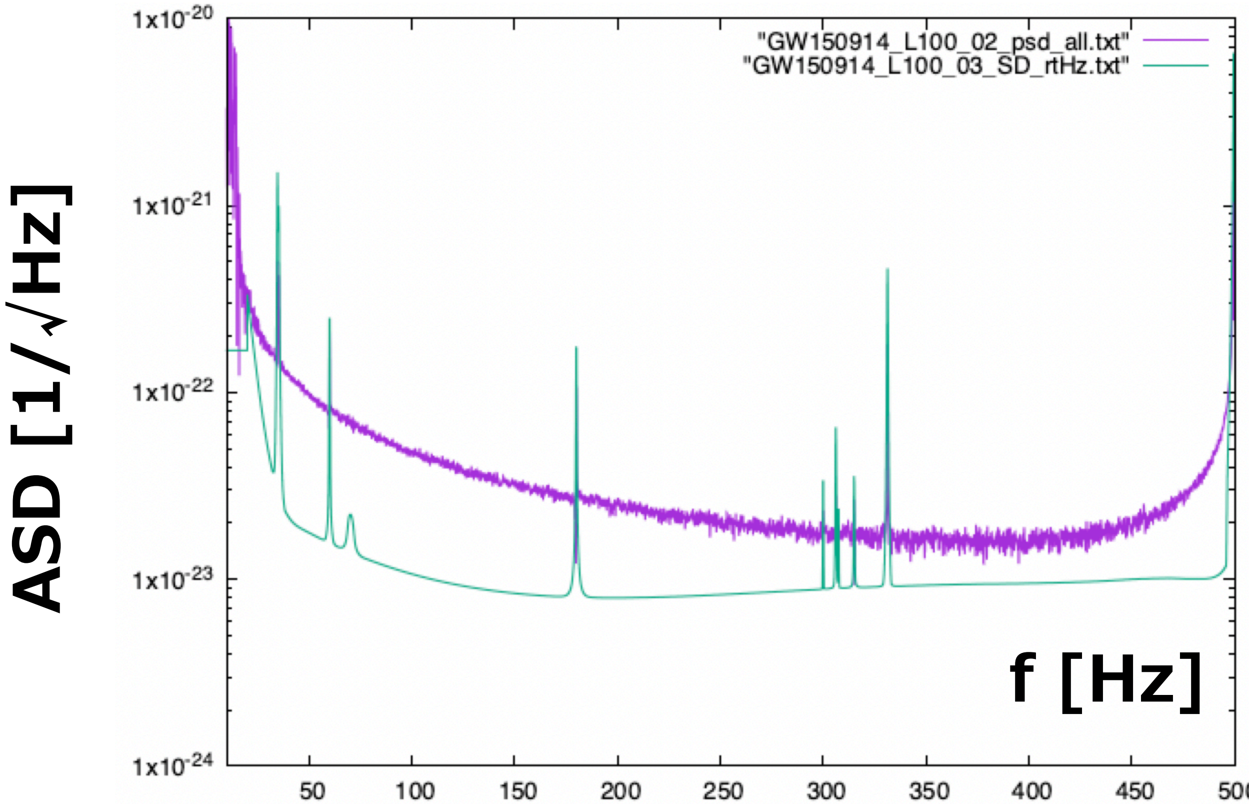

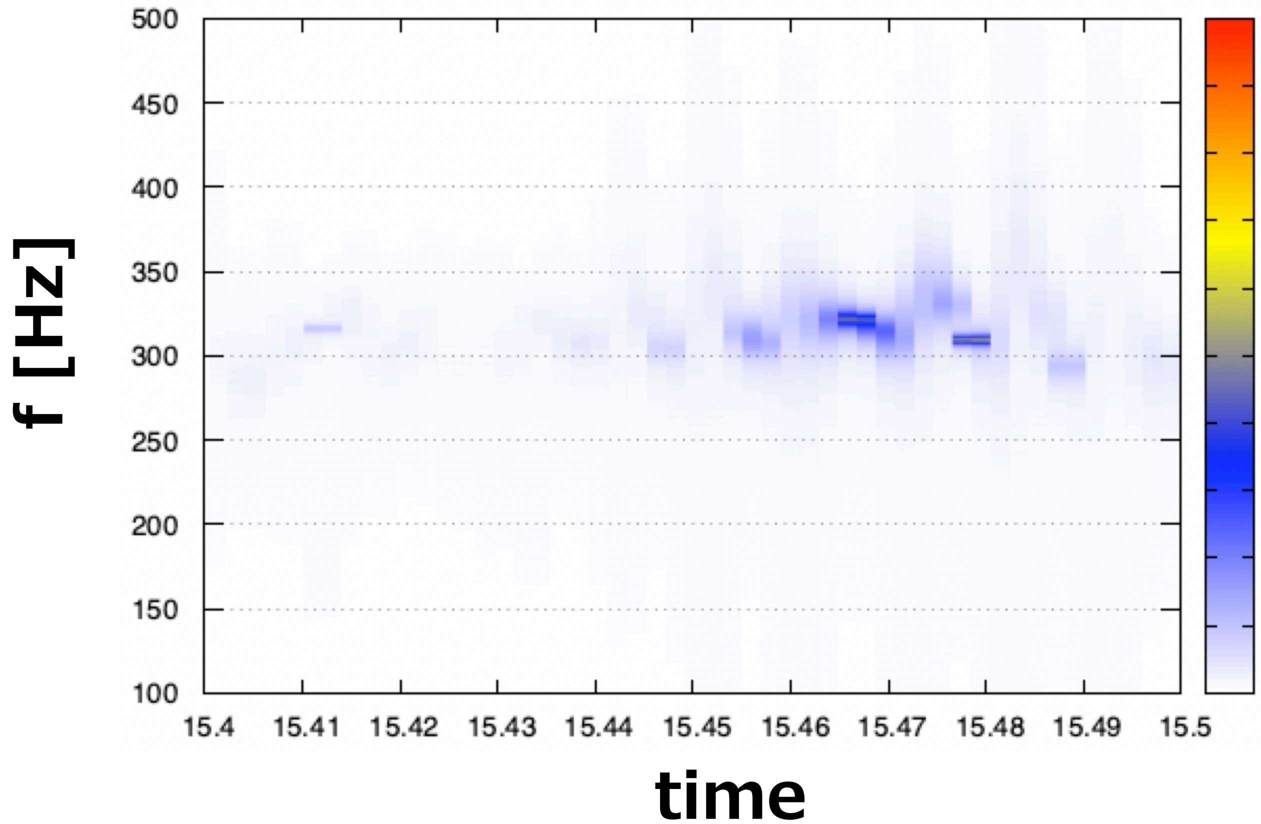

GW150914

LV paper ▶ $(M, a) = (63.1^{+3.4}_{-3.0}, 0.69^{+0.05}_{-0.04})$

f_{QNM} ▶
$f_{220} = 271.8$ Hz, $f_{221} = 266.0$ Hz, $f_{222} = 254.7$ Hz
$f_{210} = 380.7$ Hz, $f_{211} = 225.7$ Hz, $f_{200} = 252.8$ Hz
$f_{330} = 430.9$ Hz, $f_{331} = 427.4$ Hz, $f_{332} = 421.1$ Hz
$f_{320} = 387.9$ Hz, $f_{310} = 351.1$ Hz, $f_{300} = 320.3$ Hz

Hanford (SNR=20.6)

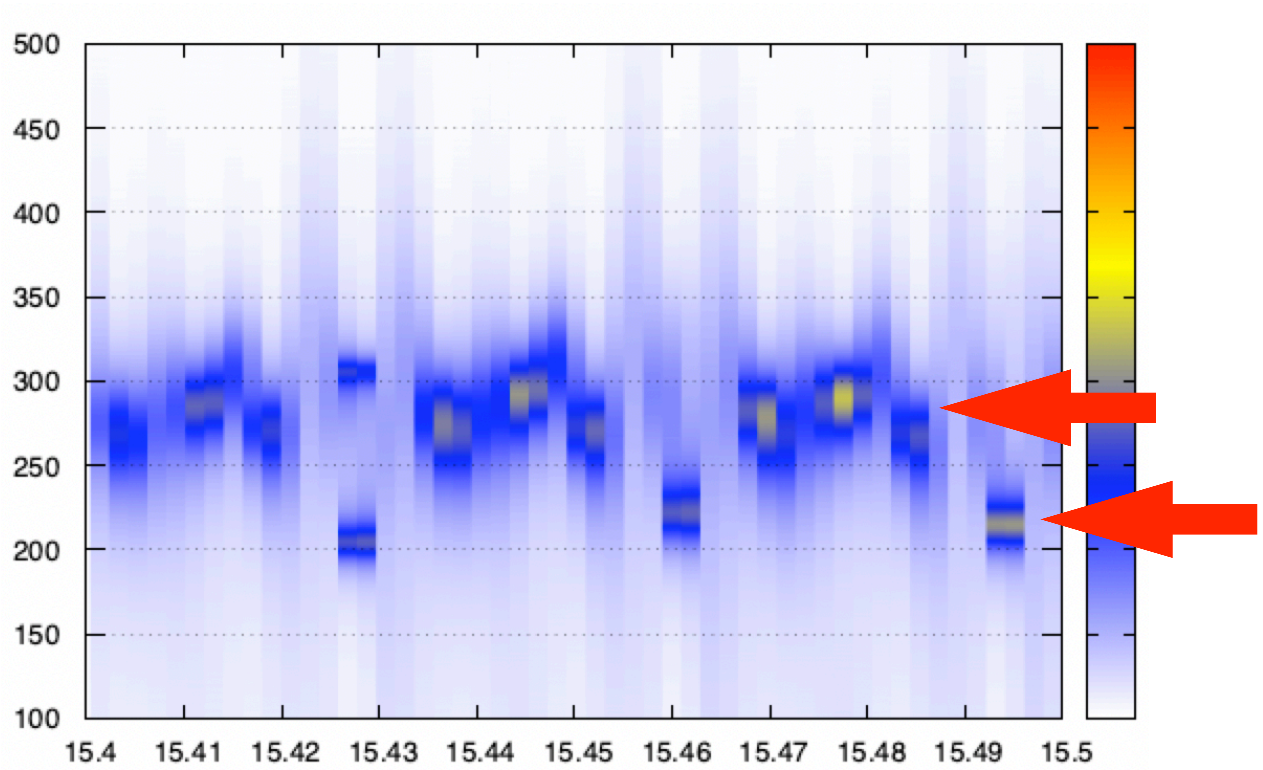

Livingston (SNR=14.2)

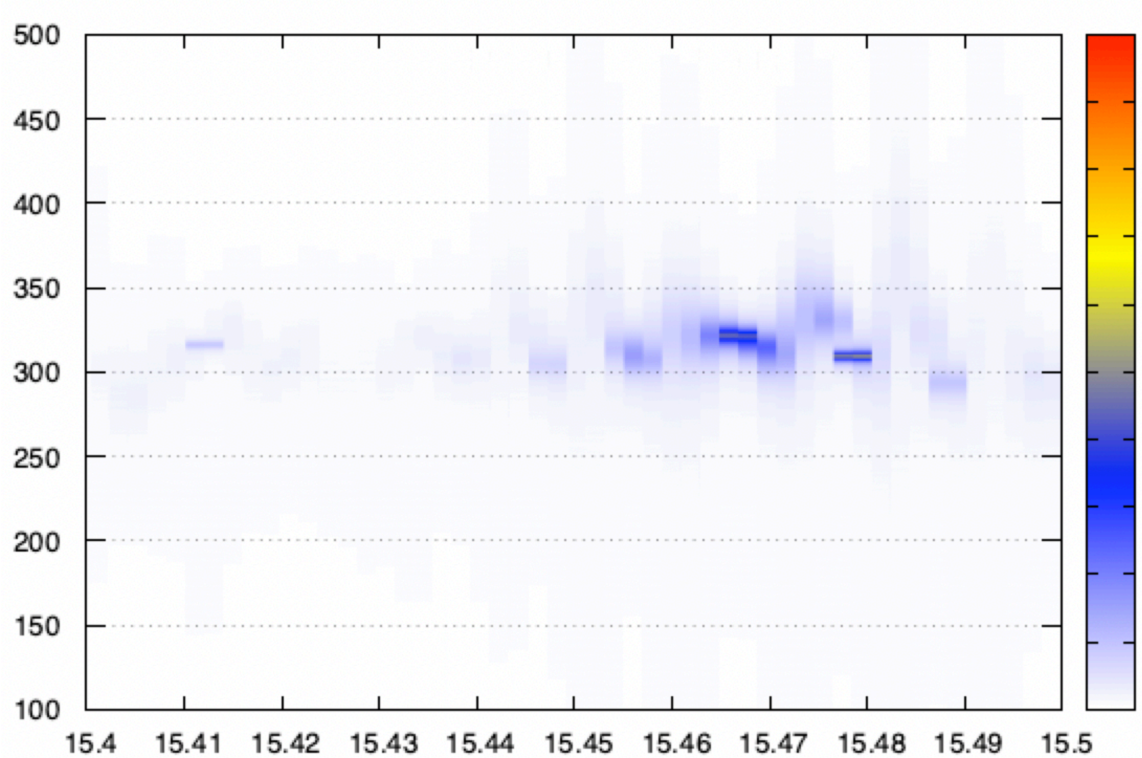

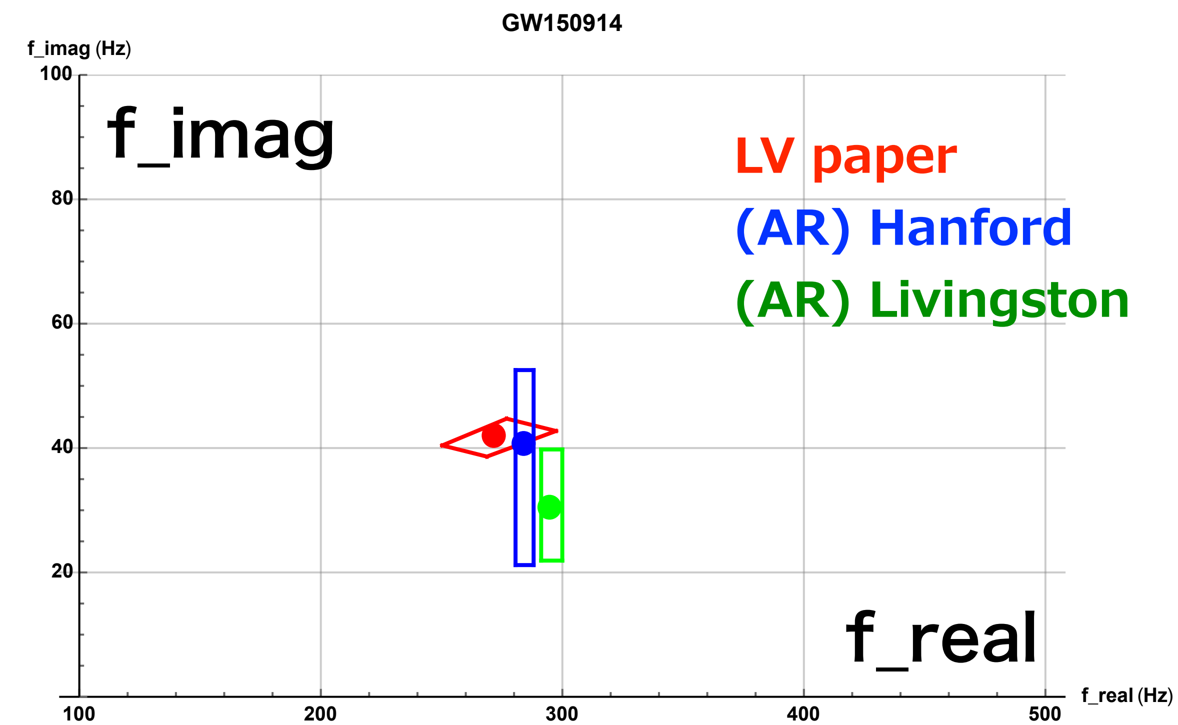

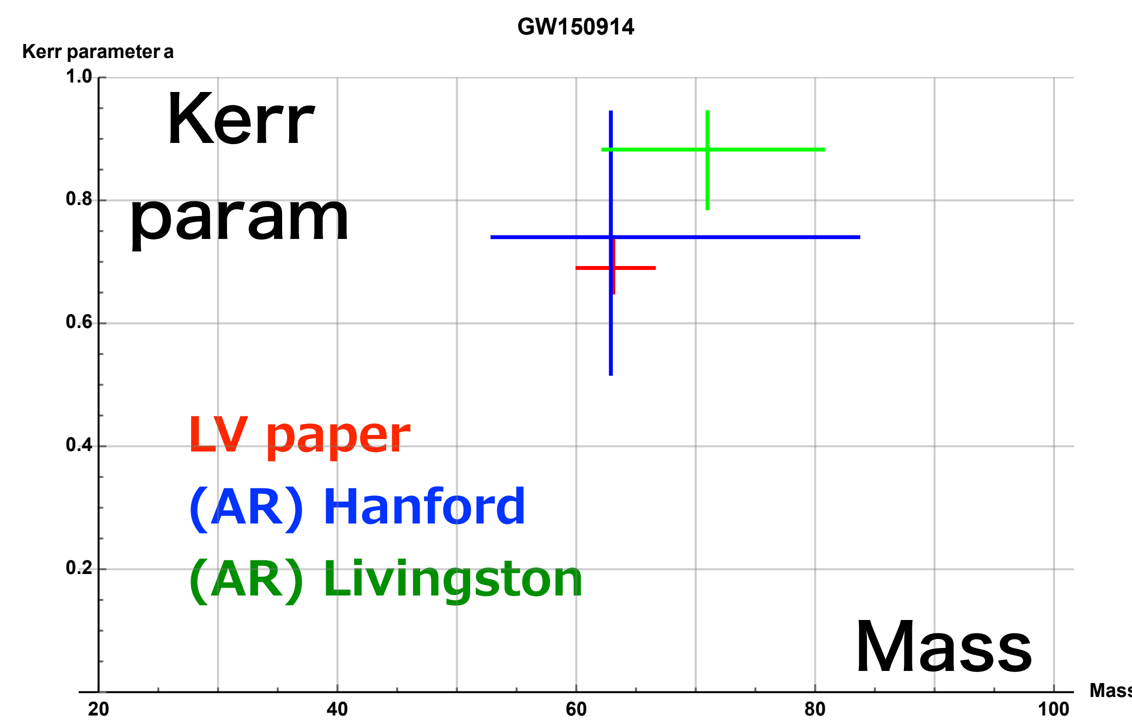

GW151012

Hanford (SNR=6.4)

H1n6_SpectrogramAR

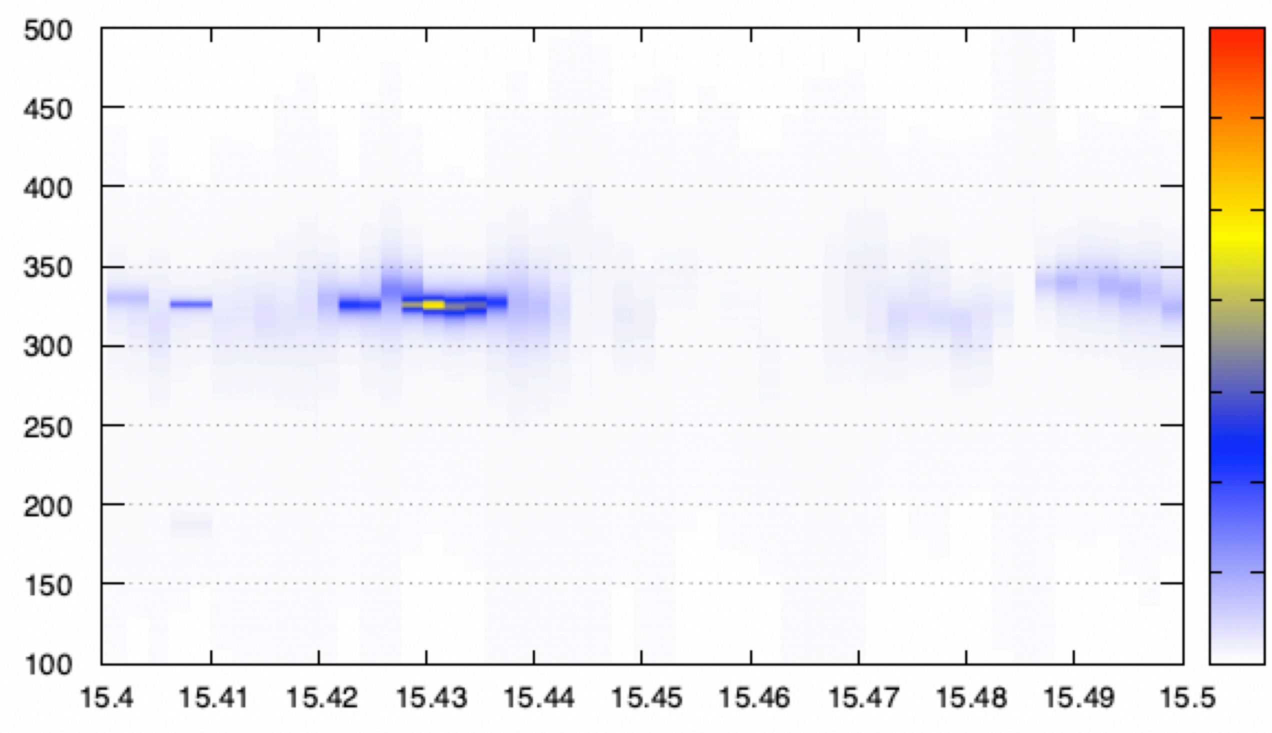

Livingston (SNR=5.8)

L1n6_SpectrogramAR

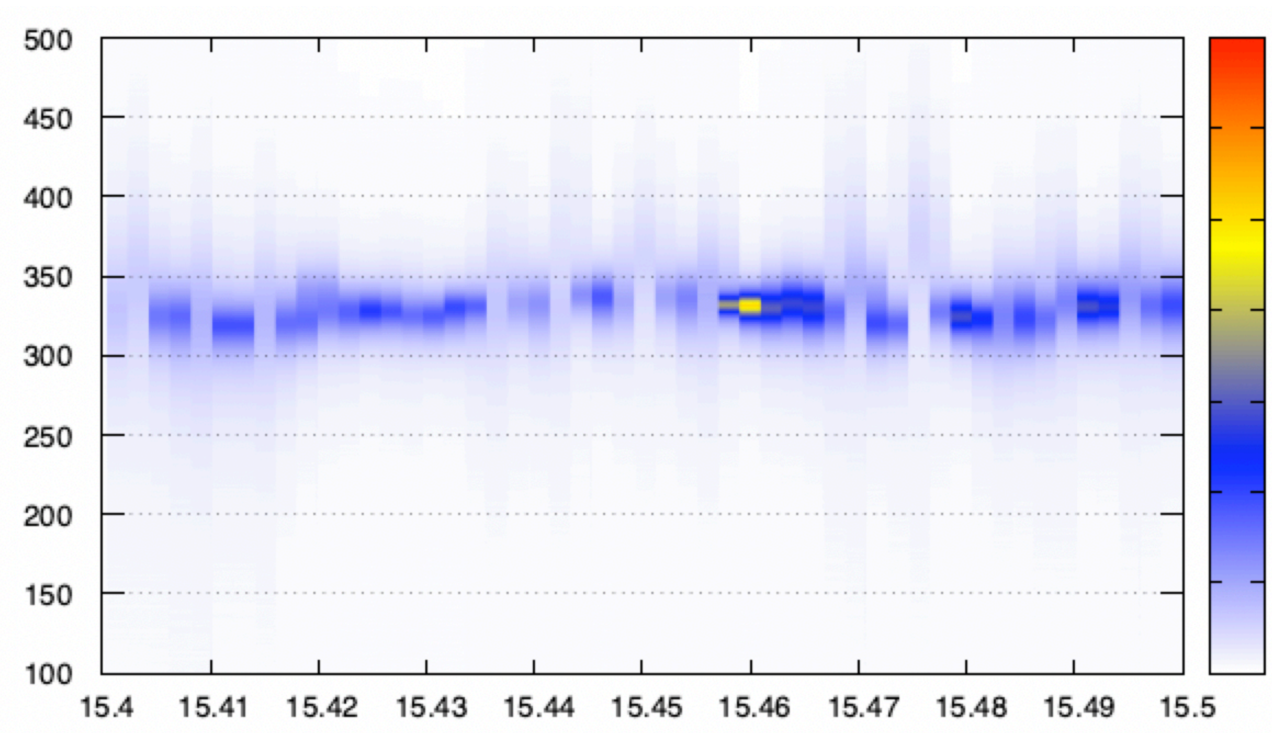

LV paper ▶ $(M, a) = (35.6^{+10.8}_{-3.8}, 0.67^{+0.13}_{-0.11})$

$f_{\rm QNM}$ ▶

$f_{220} = 474.4$ Hz, $f_{221} = 463.6$ Hz, $f_{222} = 442.7$ Hz
$f_{210} = 678.3$ Hz, $f_{211} = 396.3$ Hz, $f_{200} = 449.0$ Hz
$f_{330} = 752.8$ Hz, $f_{331} = 746.3$ Hz, $f_{332} = 734.4$ Hz
$f_{320} = 680.8$ Hz, $f_{310} = 618.8$ Hz, $f_{300} = 566.6$ Hz

Mass is small.
$f_{\rm QNM}$ is out of range.

GW151226

Hanford (SNR=9.8)

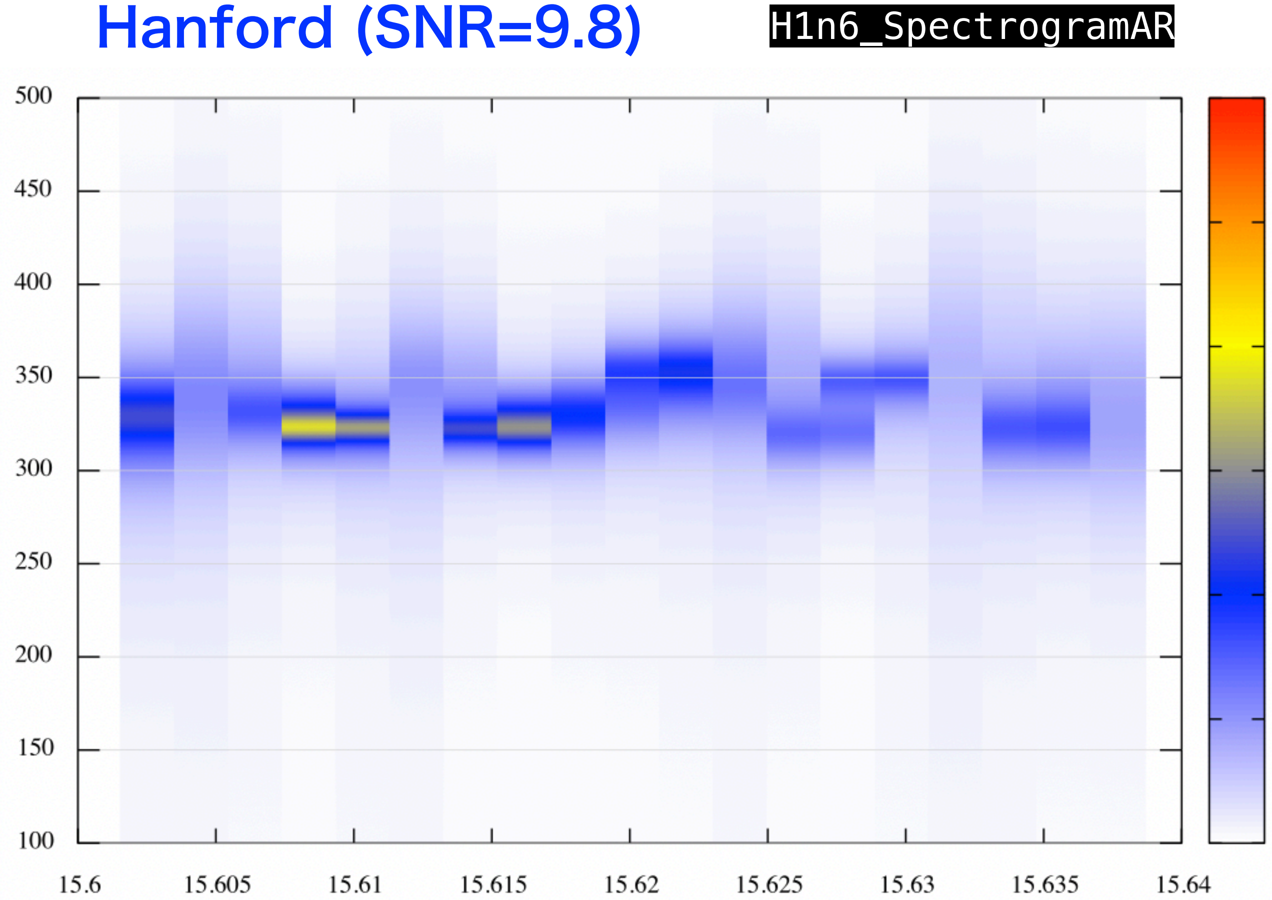

Livingston (SNR=6.9)

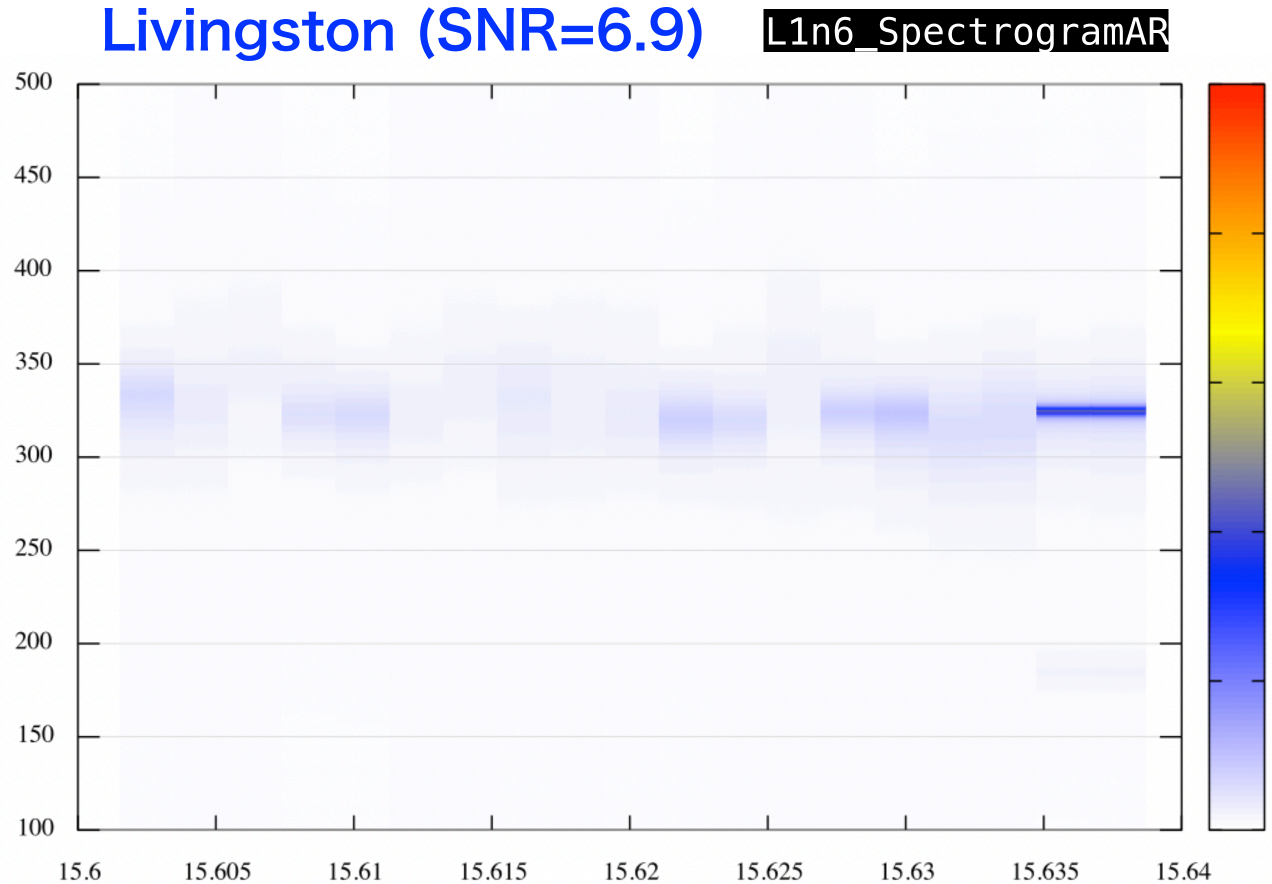

LV paper ▶ $(M, a) = (20.5^{+6.4}_{-1.5}, 0.74^{+0.07}_{-0.05})$

$f_{\rm QNM}$ ▶

$f_{220} = 871.8$ Hz, $f_{221} = 856.5$ Hz, $f_{222} = 825.9$ Hz
$f_{210} = 1156.$ Hz, $f_{211} = 712.3$ Hz, $f_{200} = 773.6$ Hz
$f_{330} = 1379.$ Hz, $f_{331} = 1369.$ Hz, $f_{332} = 1353.$ Hz
$f_{320} = 1226.$ Hz, $f_{310} = 1097.$ Hz, $f_{300} = 991.8$ Hz

Mass is small.

$f_{\rm QNM}$ is out of range.

GW170104

Hanford (SNR=9.5)

H1n6_SpectrogramAR

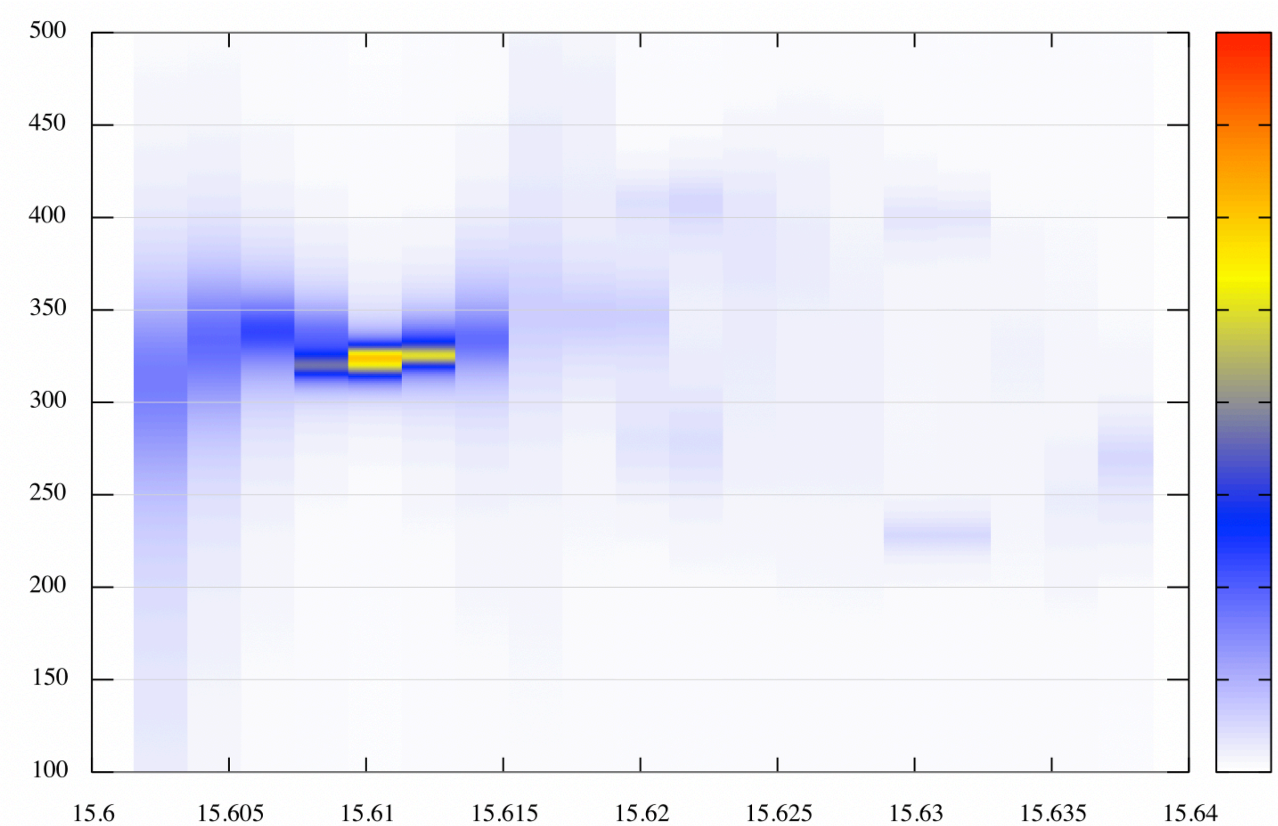

LV paper ▶

$$(M, a) = (48.9^{+5.1}_{-4.0}, 0.66^{+0.08}_{-0.11})$$

f_{QNM} ▶

$f_{220} = 342.8$ Hz, $f_{221} = 334.7$ Hz, $f_{222} = 319.2$ Hz
$f_{210} = 495.0$ Hz, $f_{211} = 287.2$ Hz, $f_{200} = 327.2$ Hz
$f_{330} = 544.2$ Hz, $f_{331} = 539.3$ Hz, $f_{332} = 530.5$ Hz
$f_{320} = 493.3$ Hz, $f_{310} = 449.3$ Hz, $f_{300} = 412.0$ Hz

Livingston (SNR=9.9)

L1n6_SpectrogramAR

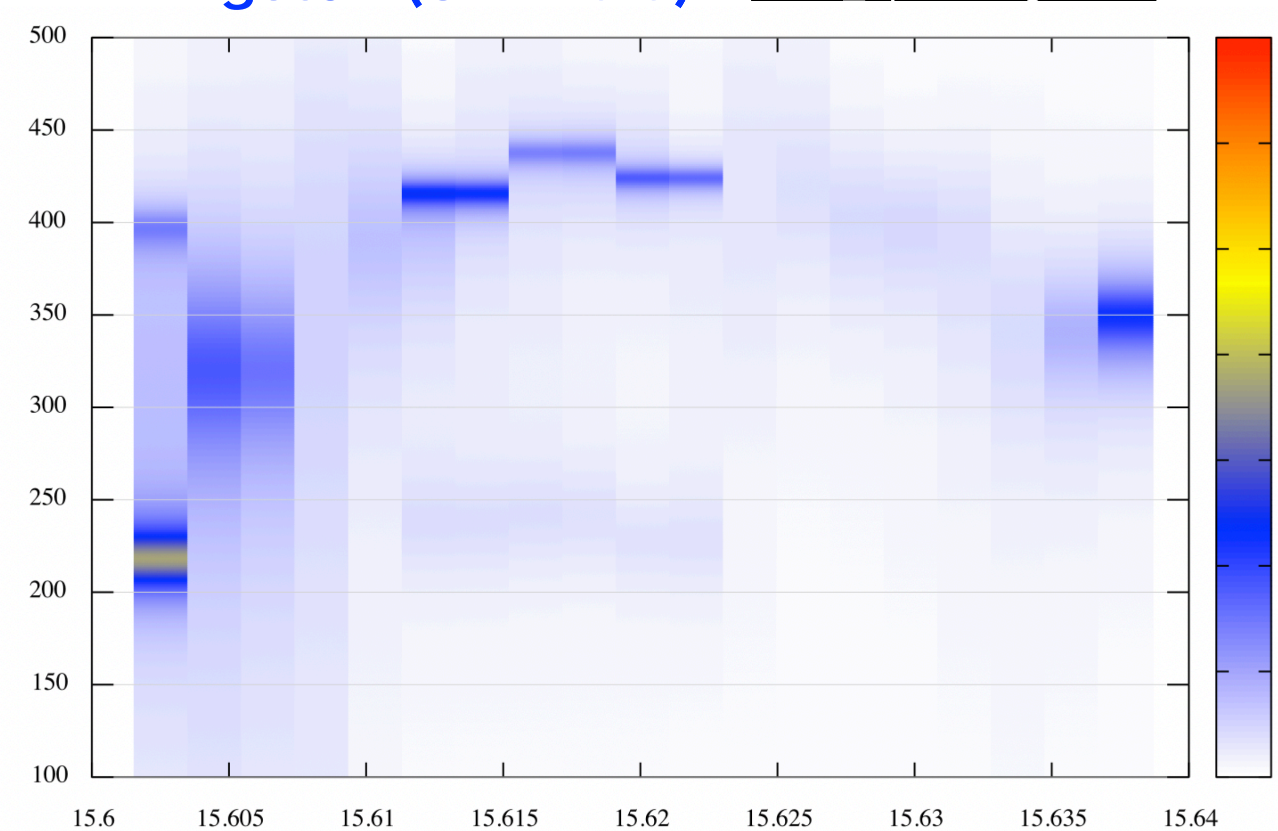

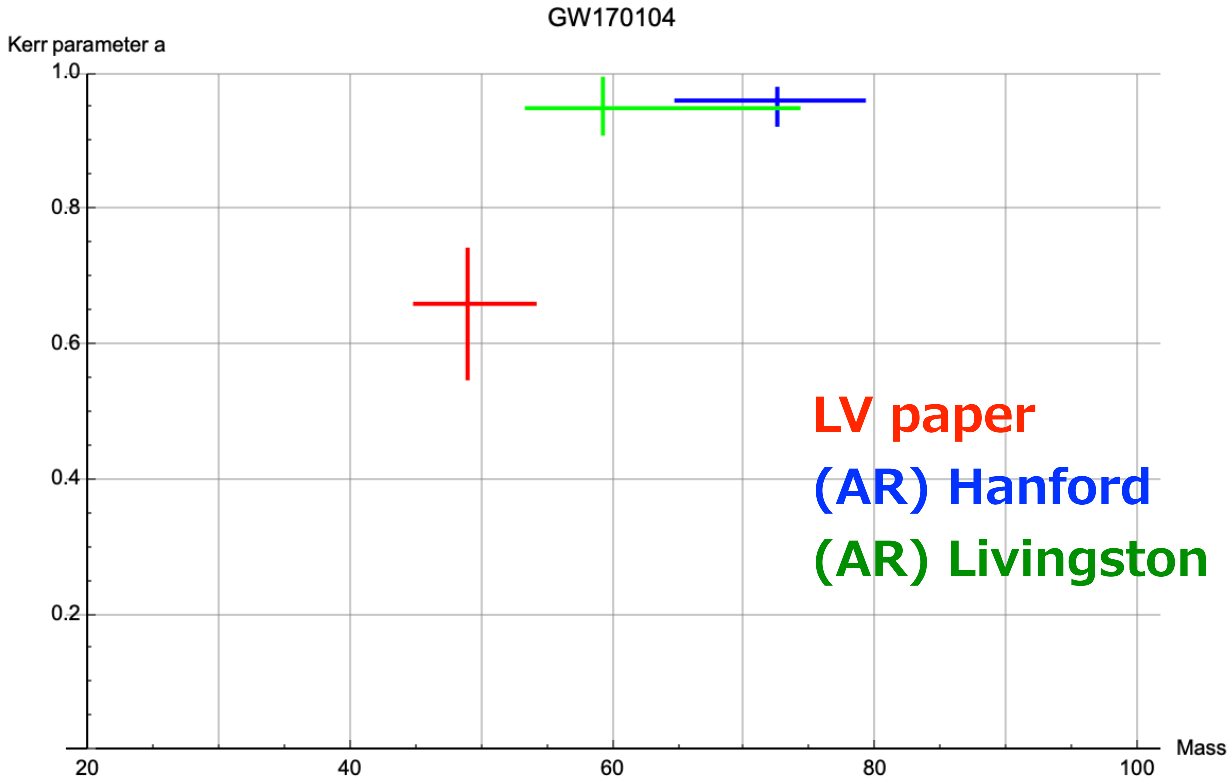

GW170608

Hanford (SNR=12.1)

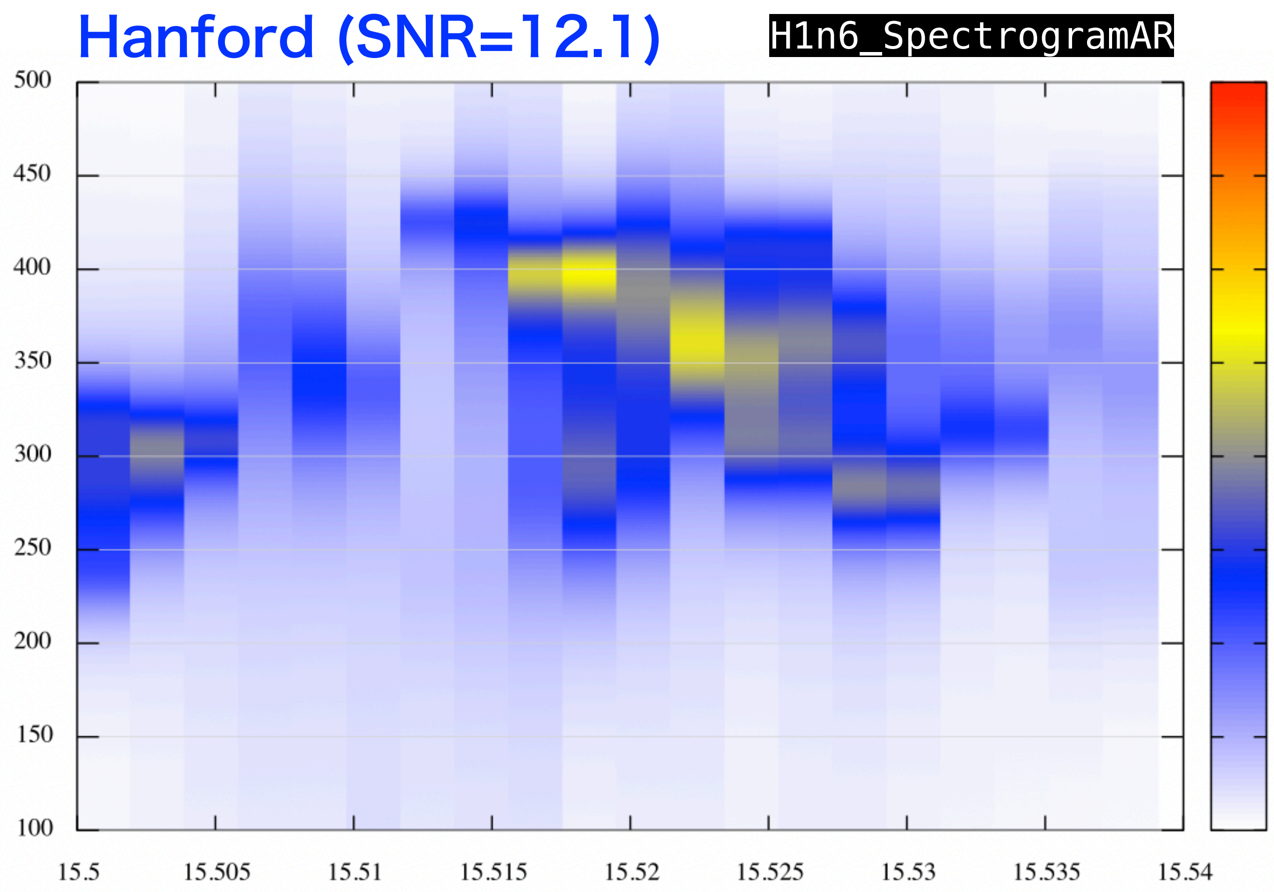

Livingston (SNR=9.2)

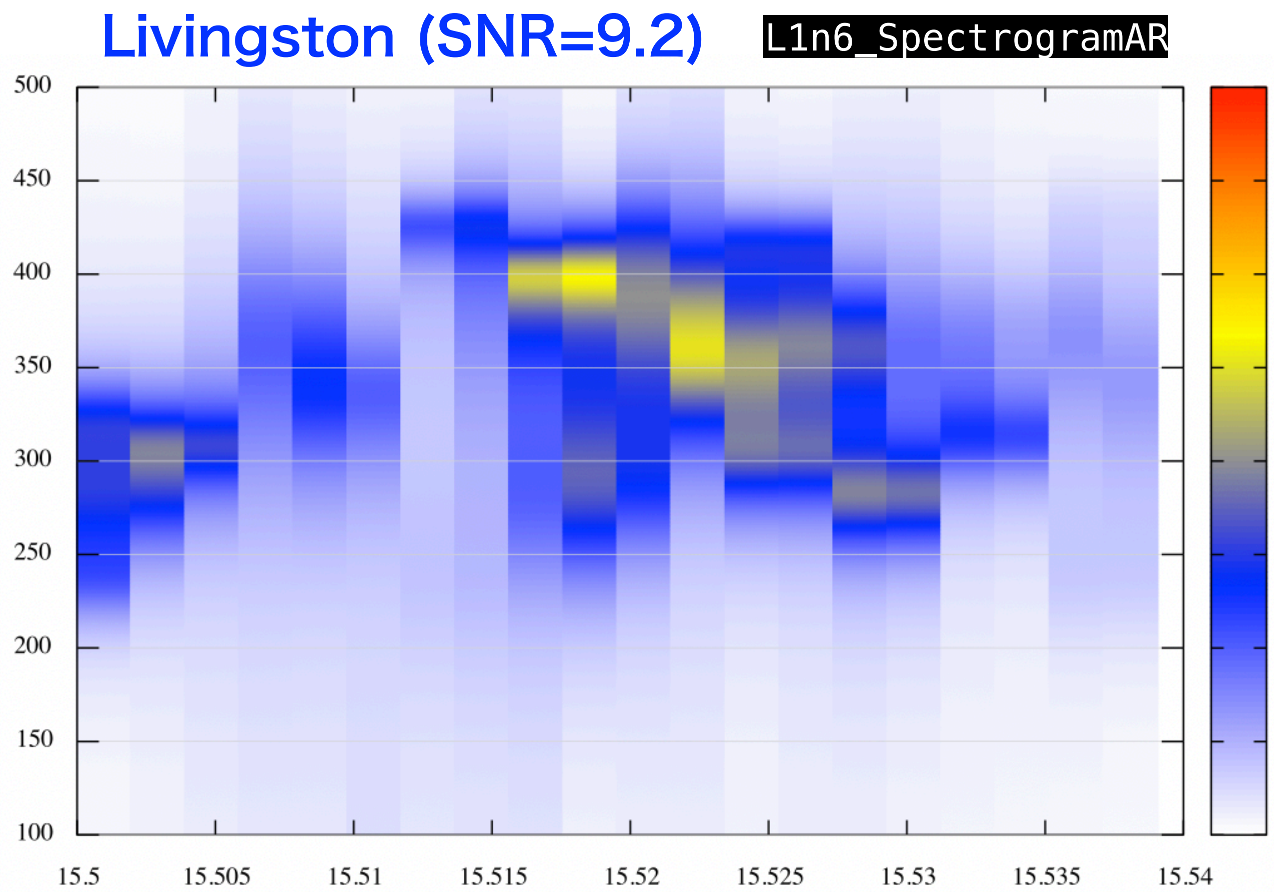

LV paper ▶ $(M, a) = (17.8^{+3.4}_{-0.7}, 0.69^{+0.04}_{-0.04})$

f_{QNM} ▶

$f_{220} = 963.5$ Hz, $f_{221} = 942.9$ Hz, $f_{222} = 902.9$ Hz
$f_{210} = 1350.$ Hz, $f_{211} = 800.2$ Hz, $f_{200} = 896.1$ Hz
$f_{330} = 1528.$ Hz, $f_{331} = 1515.$ Hz, $f_{332} = 1493.$ Hz
$f_{320} = 1375.$ Hz, $f_{310} = 1245.$ Hz, $f_{300} = 1136.$ Hz

Mass is small.

f_{QNM} is out of range.

GW170729

$$(M, a) = (79.5^{+14.7}_{-10.2}, 0.81^{+0.07}_{-0.13})$$

$f_{220} = 240.5$ Hz, $f_{221} = 237.5$ Hz, $f_{222} = 231.3$ Hz
$f_{210} = 291.4$ Hz, $f_{211} = 190.8$ Hz, $f_{200} = 197.6$ Hz

Hanford (SNR=5.9)

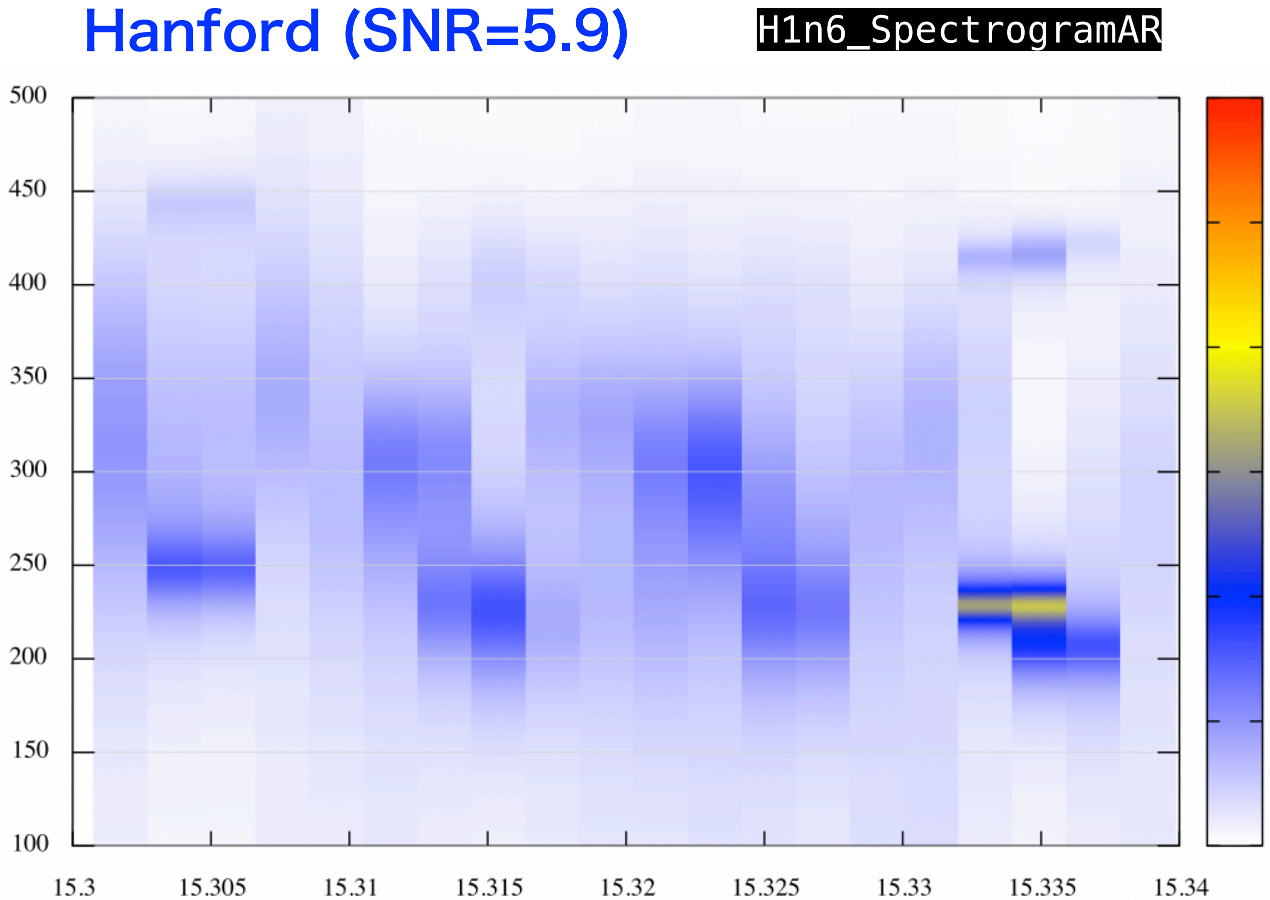

Virgo (SNR=1.7)

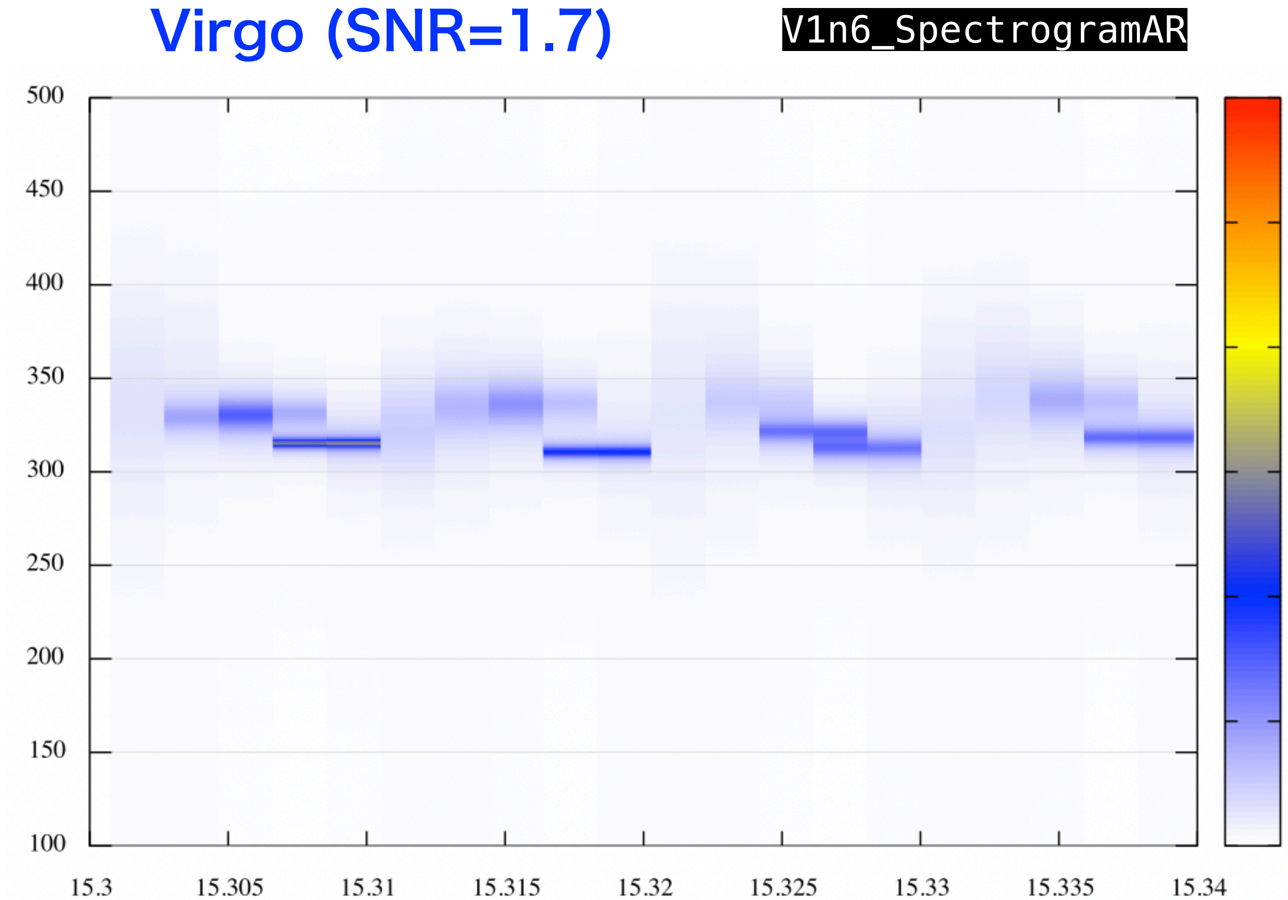

Livingston (SNR=8.3)

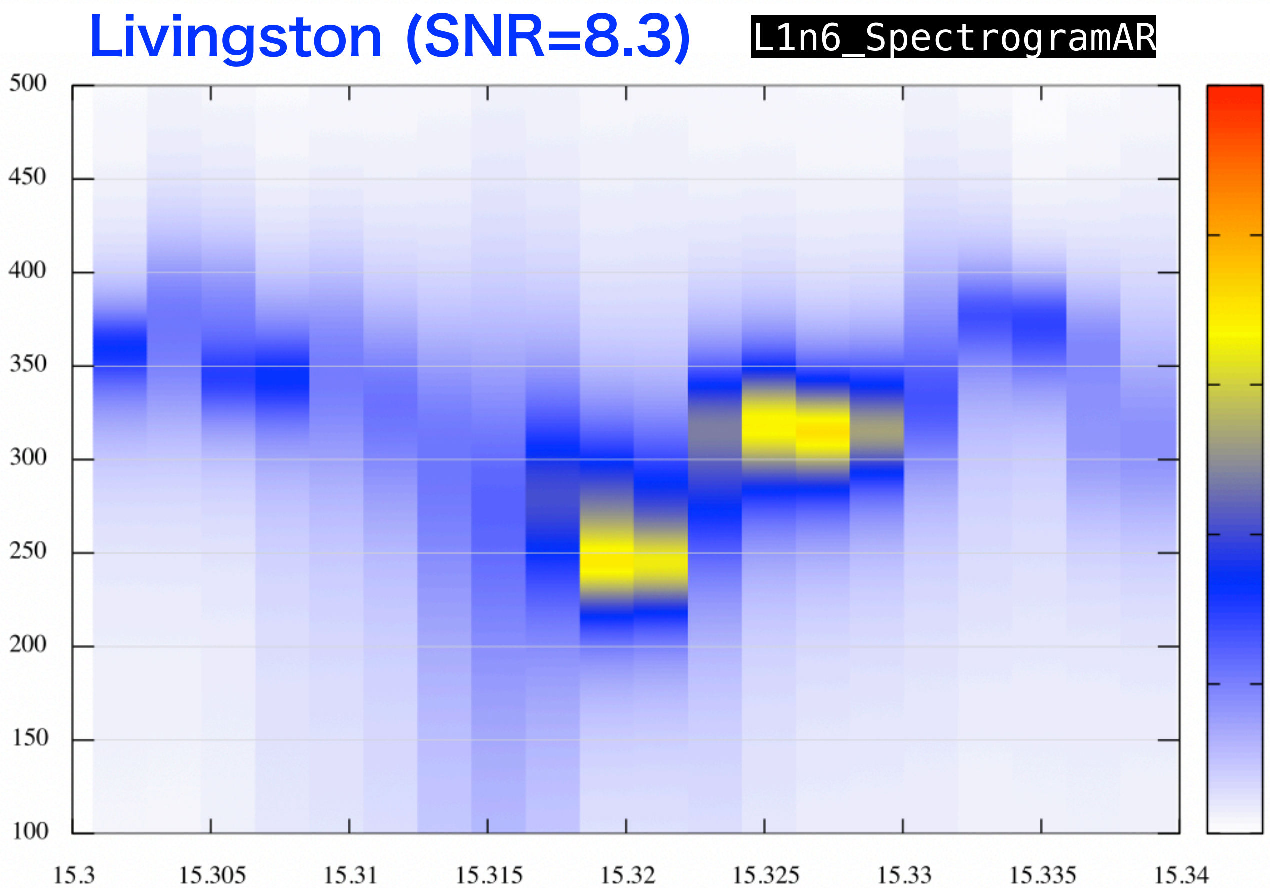

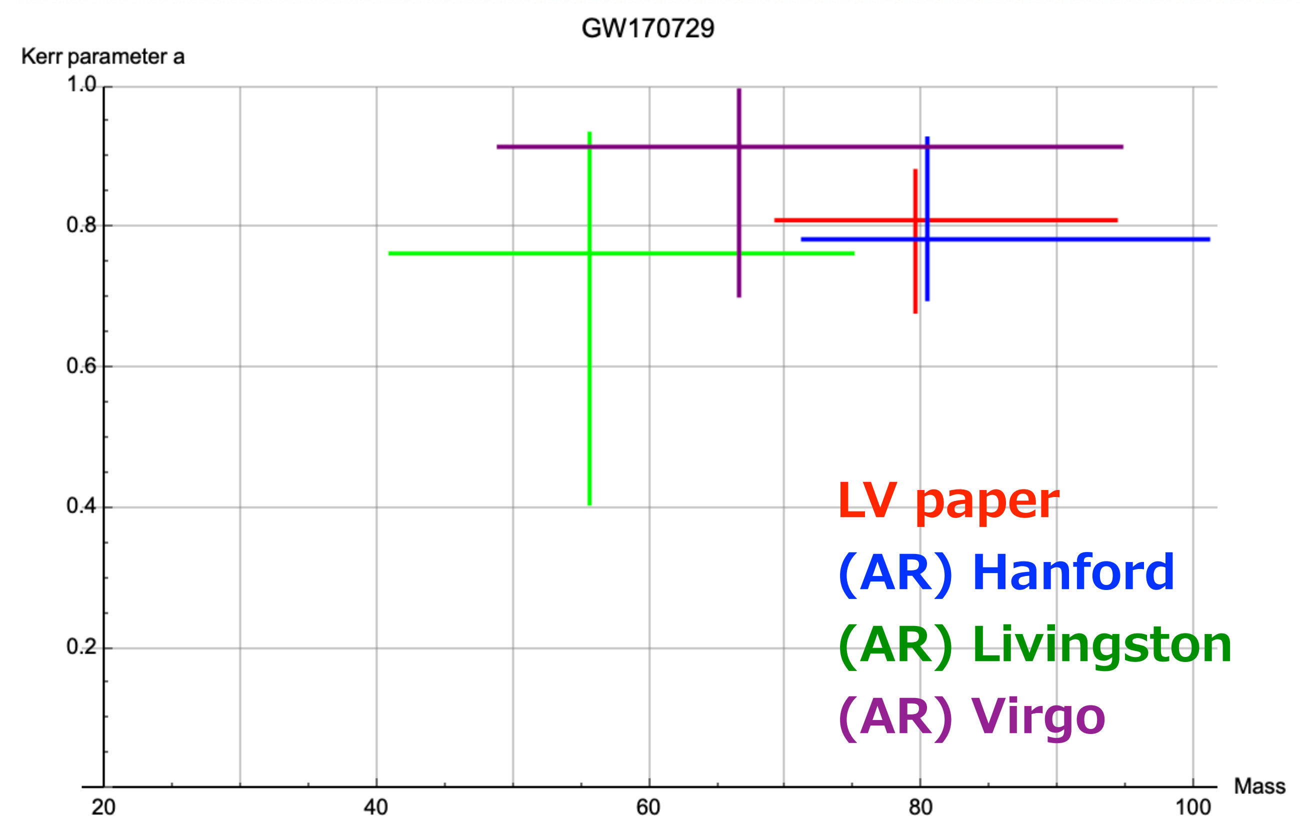

GW170809

$(M, a) = (56.3^{+5.2}_{-3.8}, 0.7^{+0.08}_{-0.09})$

$f_{220} = 307.0$ Hz, $f_{221} = 300.7$ Hz, $f_{222} = 288.4$ Hz
$f_{210} = 425.6$ Hz, $f_{211} = 254.2$ Hz, $f_{200} = 283.0$ Hz

Hanford (SNR=5.9)

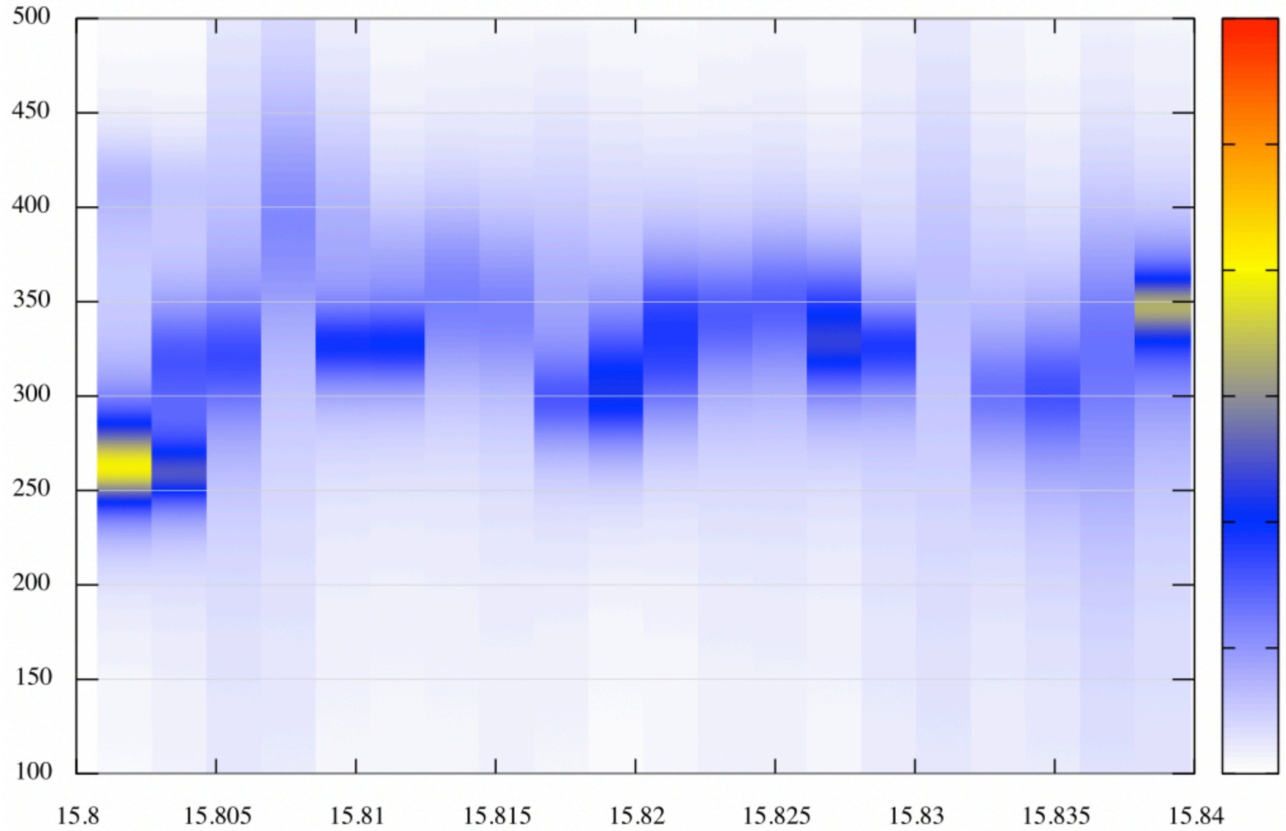

Virgo (SNR=1.1)

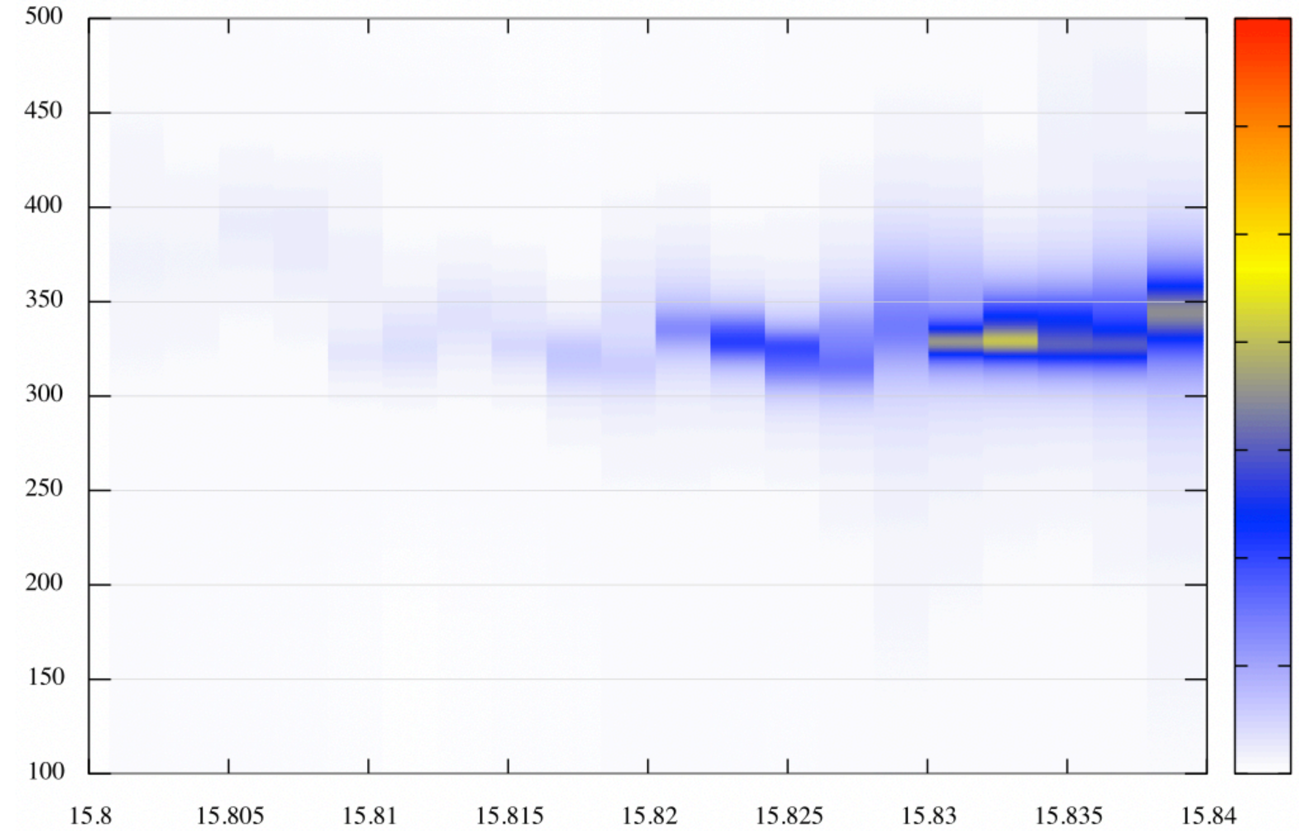

Livingston (SNR=10.7)

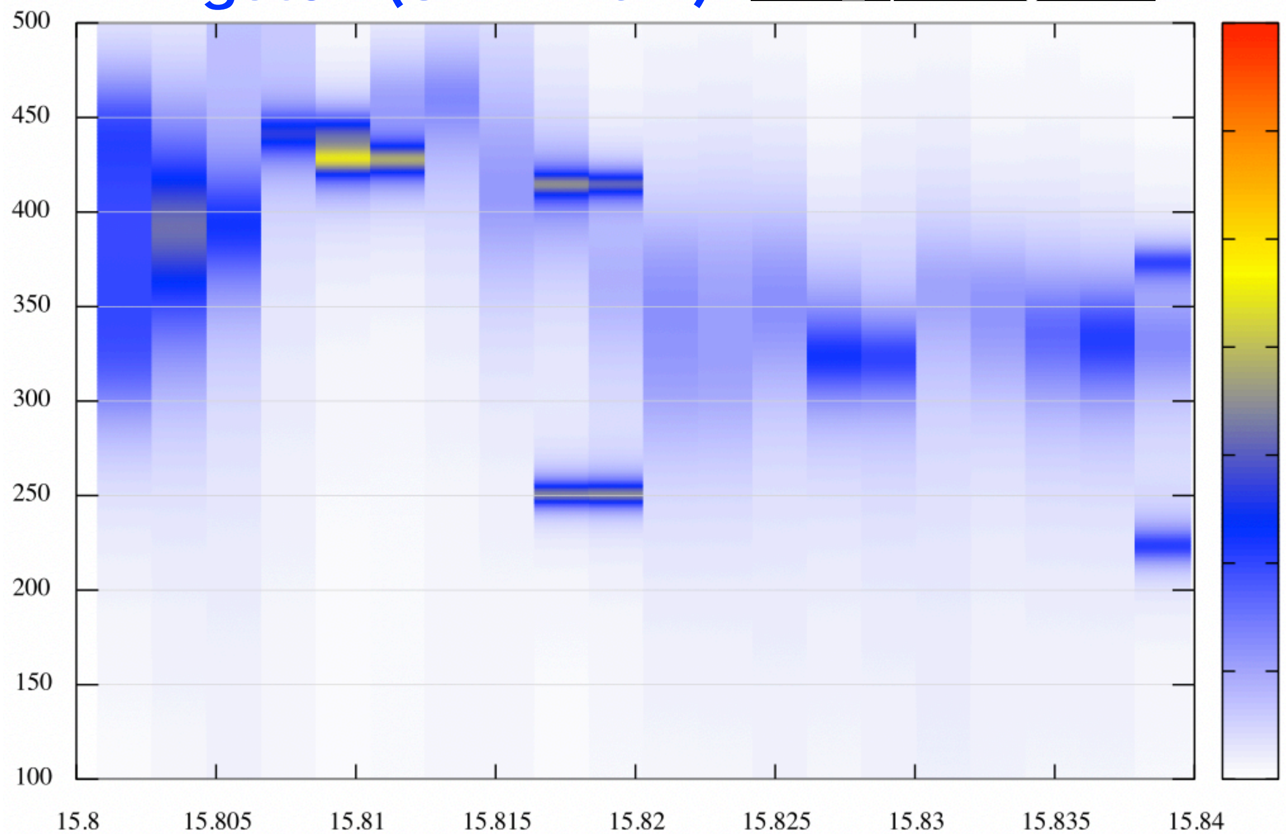

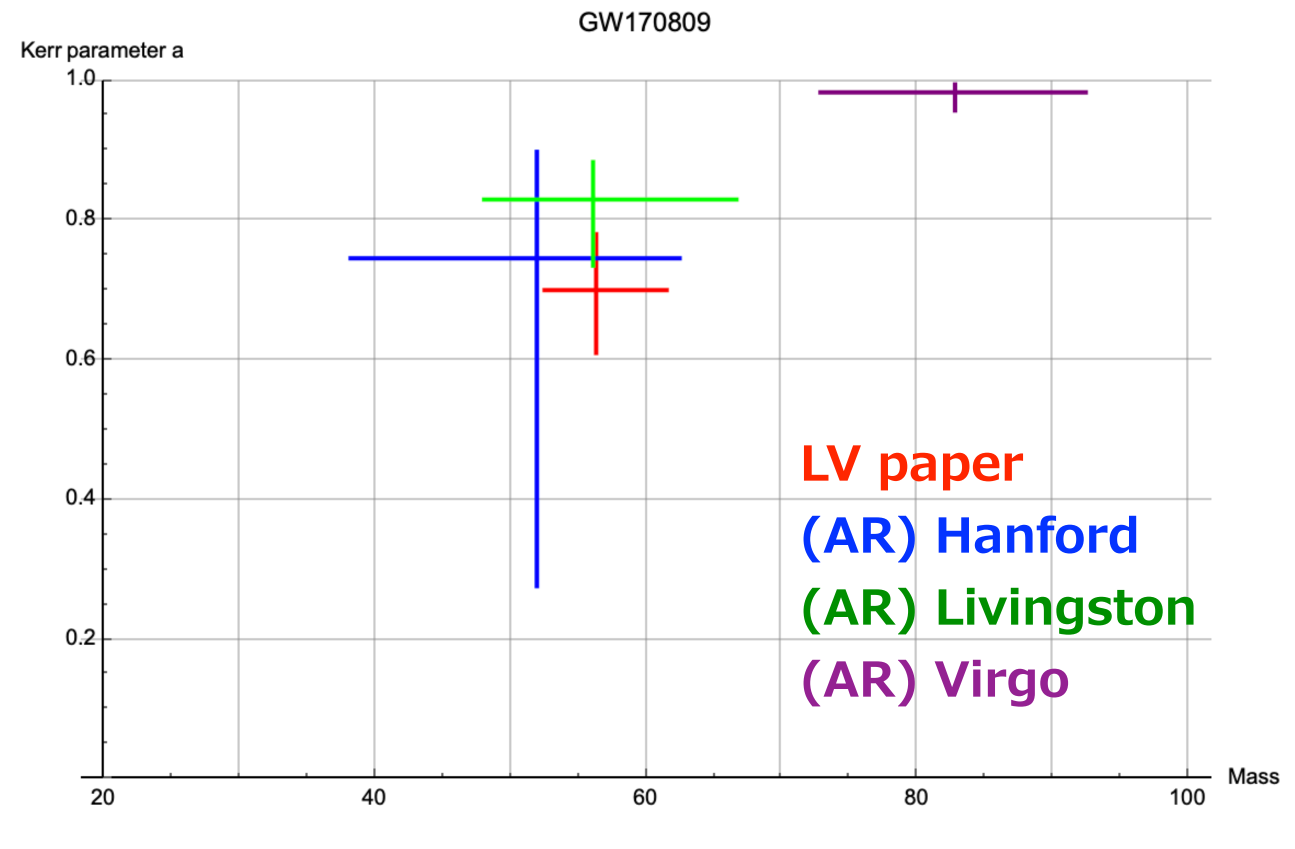

GW170814

$$(M, a) = (53.2^{+3.2}_{-2.4}, 0.72^{+0.07}_{-0.05})$$

$f_{220} = 330.3$ Hz, $f_{221} = 324.0$ Hz, $f_{222} = 311.5$ Hz
$f_{210} = 447.9$ Hz, $f_{211} = 271.7$ Hz, $f_{200} = 298.8$ Hz

Hanford (SNR=9.3)

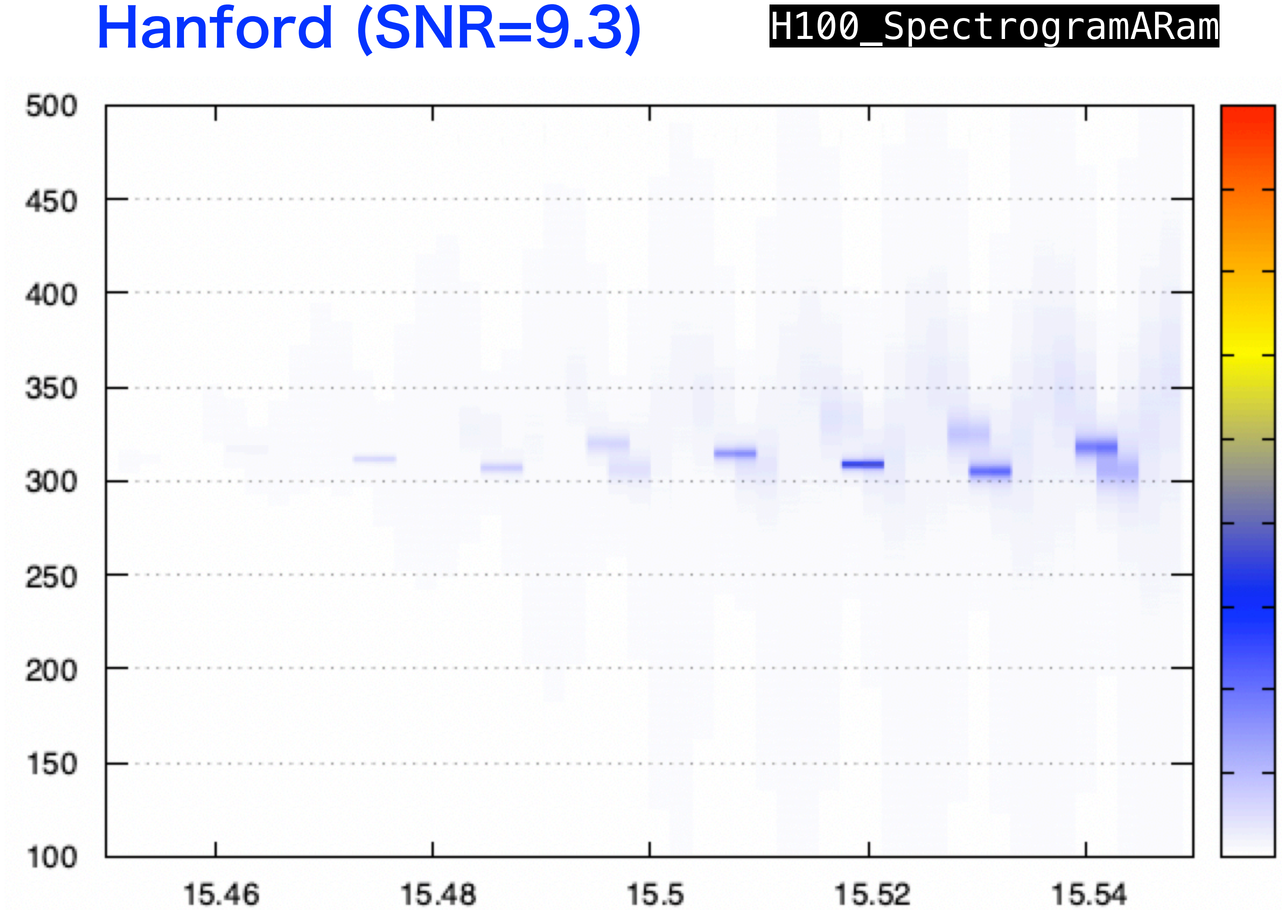

Virgo (SNR=4.1)

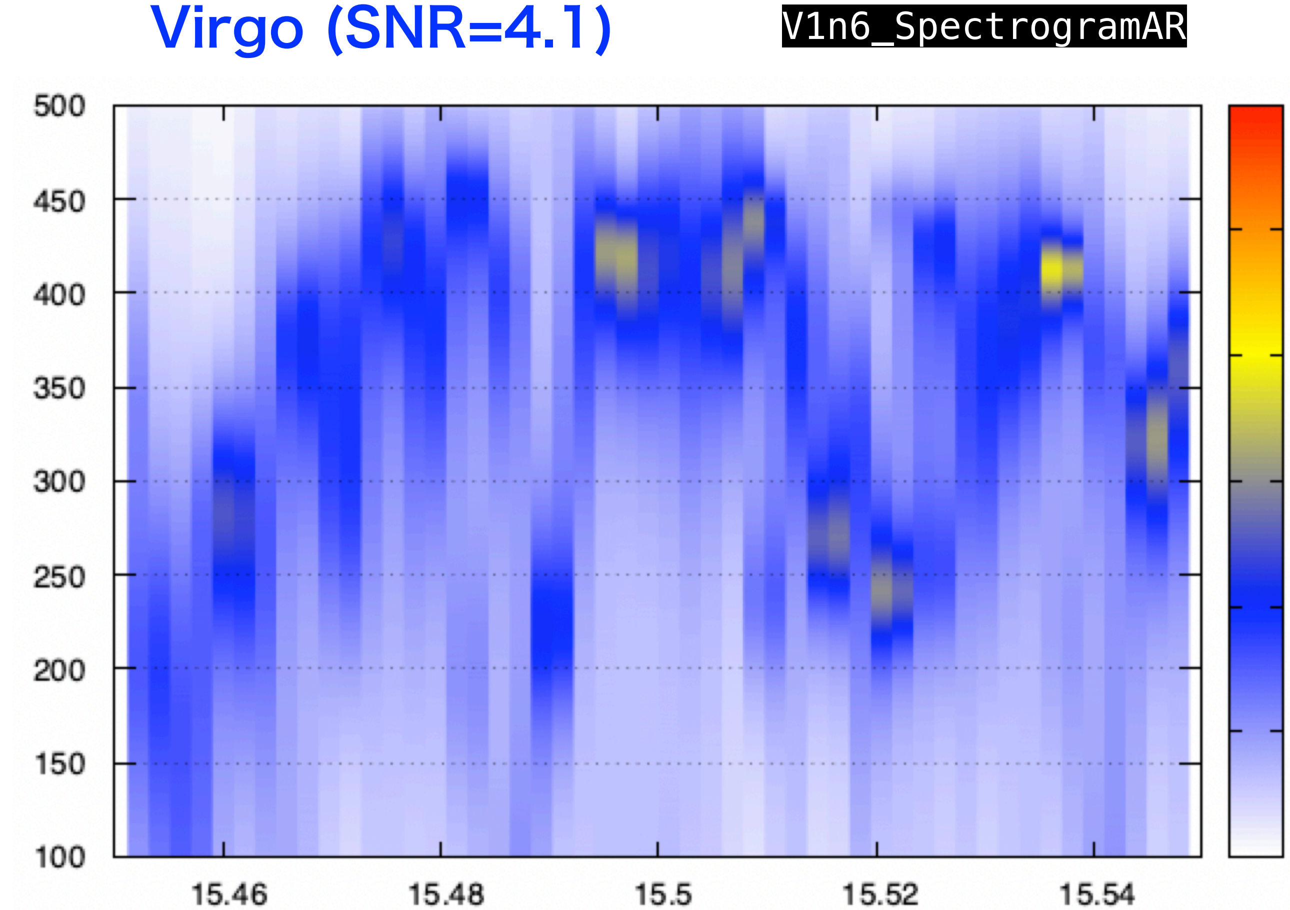

Livingston (SNR=14.3)

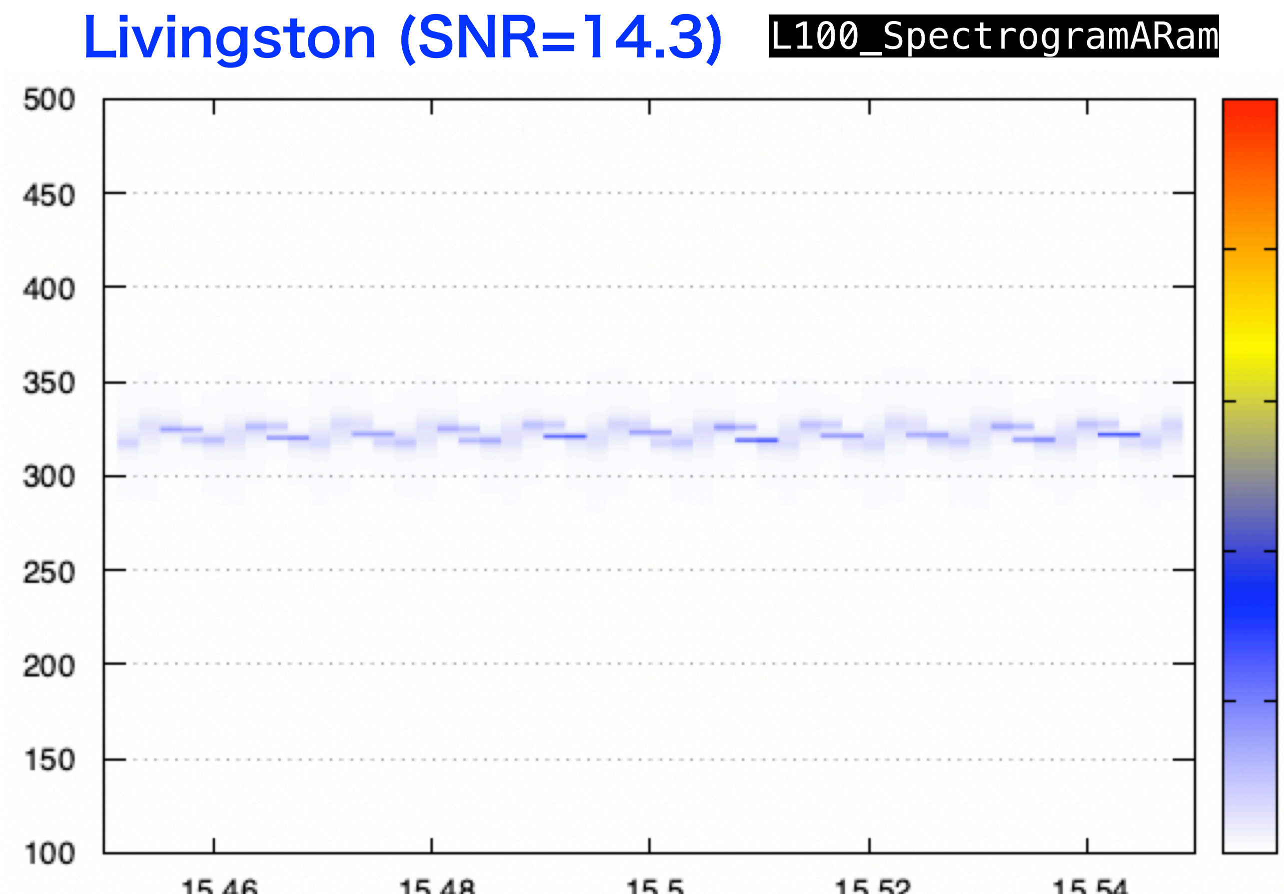

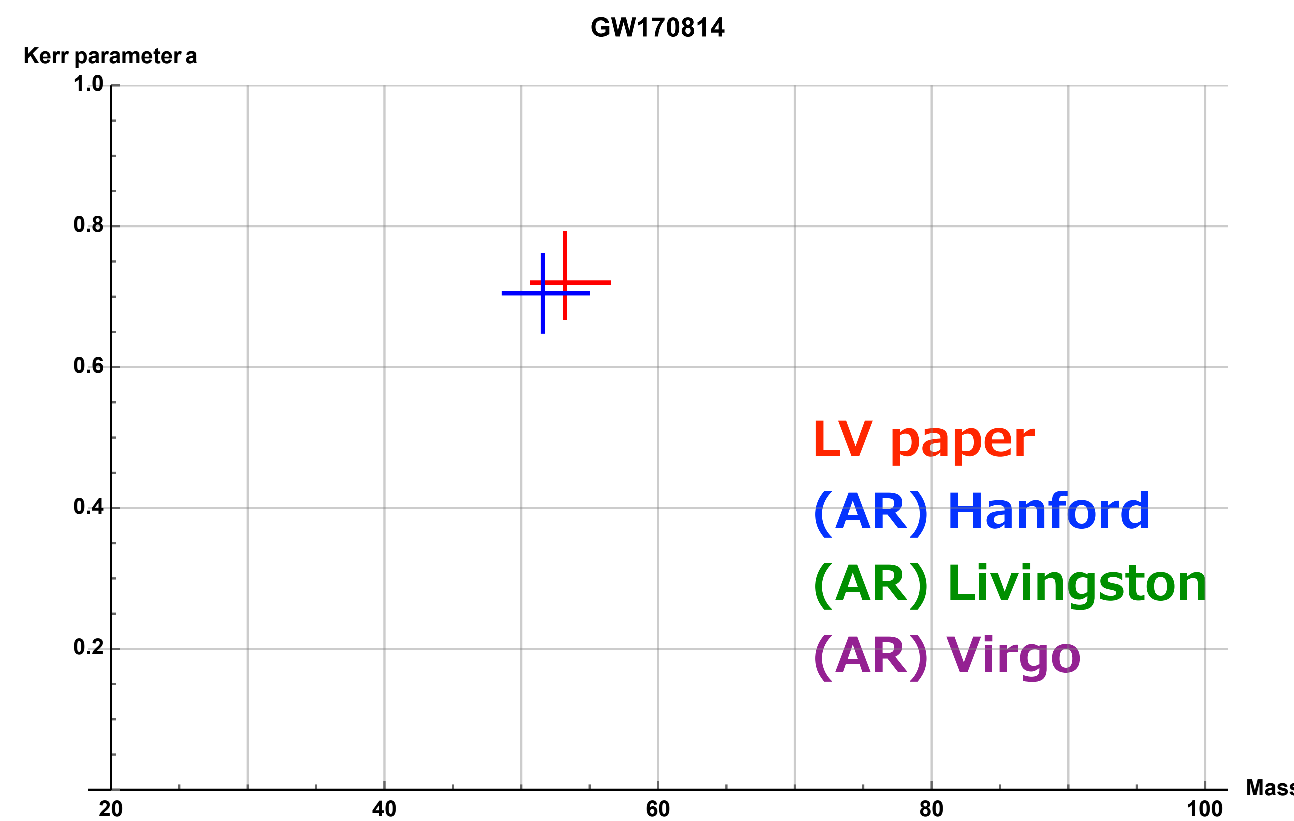

GW170818

$(M,a) = (59.4^{+4.9}_{-3.8}, 0.67^{+0.07}_{-0.08})$

$f_{220} = 307.0$ Hz, $f_{221} = 300.7$ Hz, $f_{222} = 288.4$ Hz
$f_{210} = 425.6$ Hz, $f_{211} = 254.2$ Hz, $f_{200} = 283.0$ Hz

Hanford (SNR=4.6)

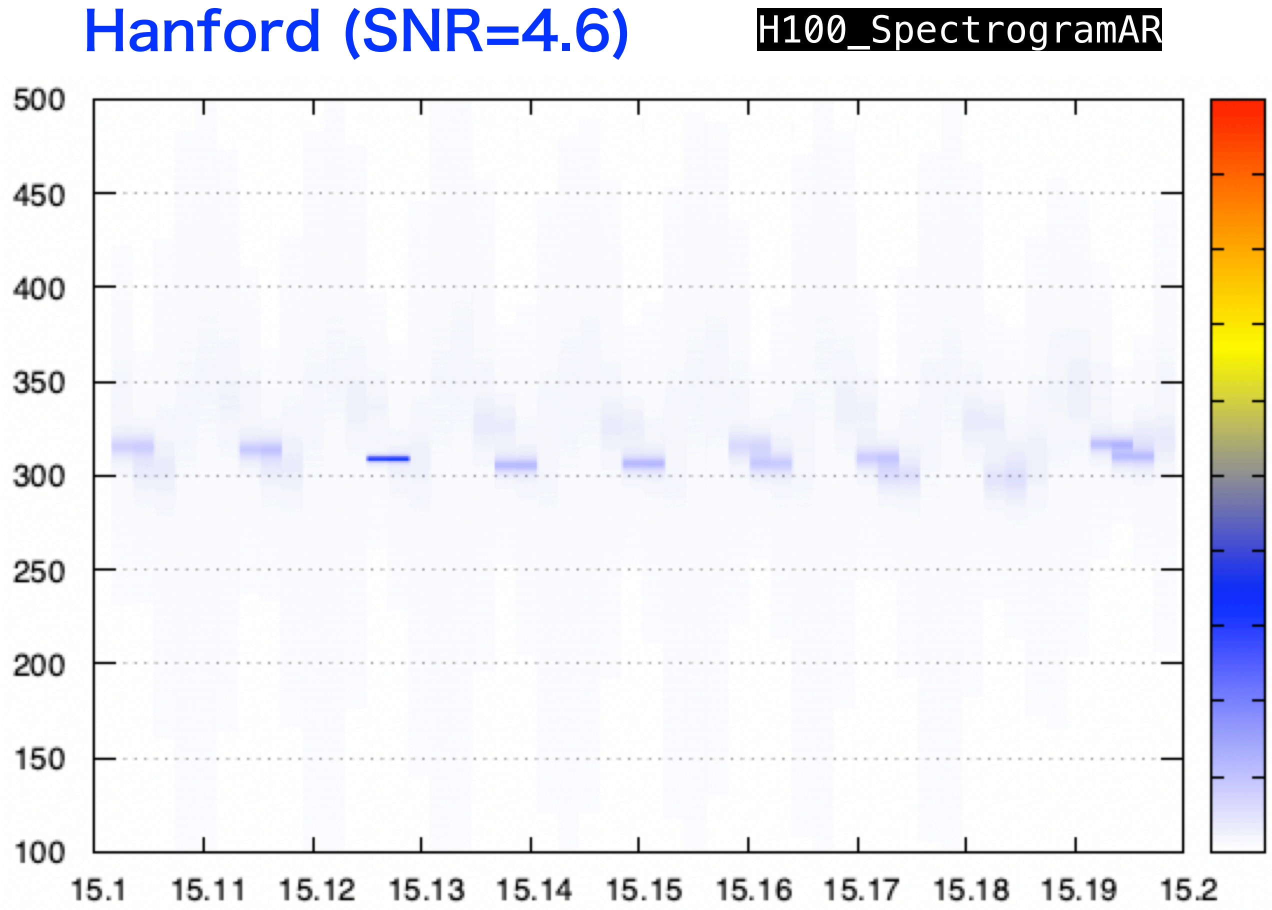

Virgo (SNR=4.2)

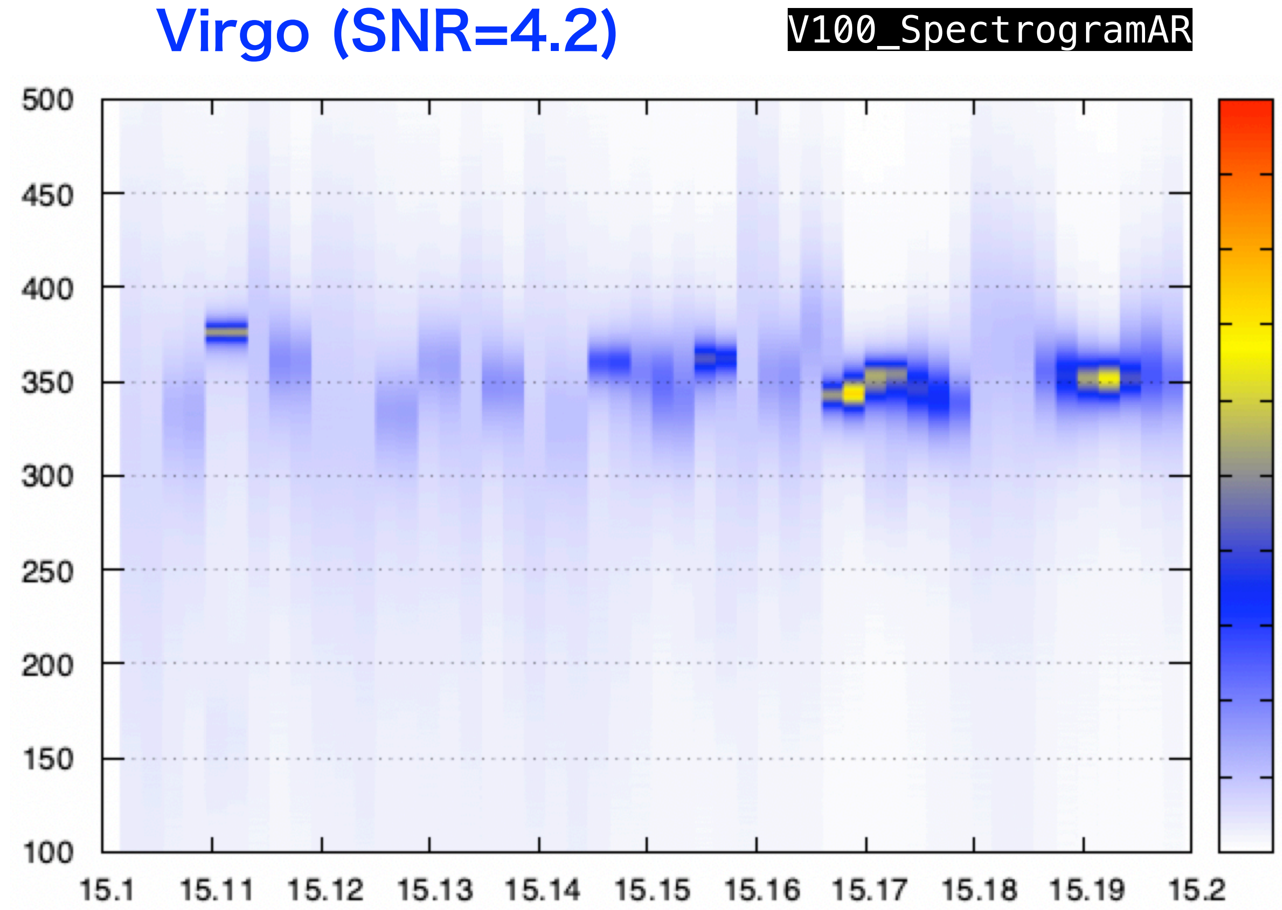

Livingston (SNR=9.7)

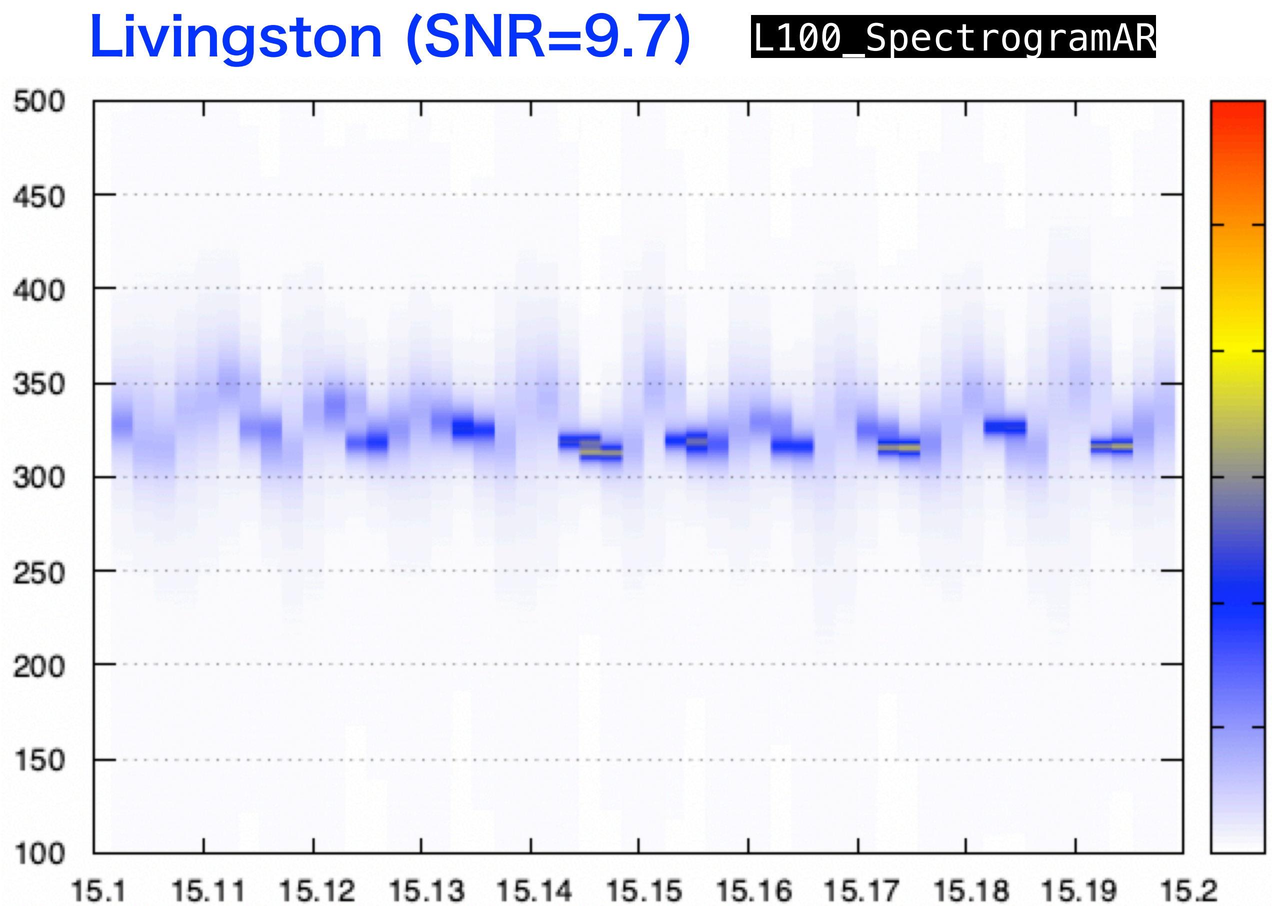

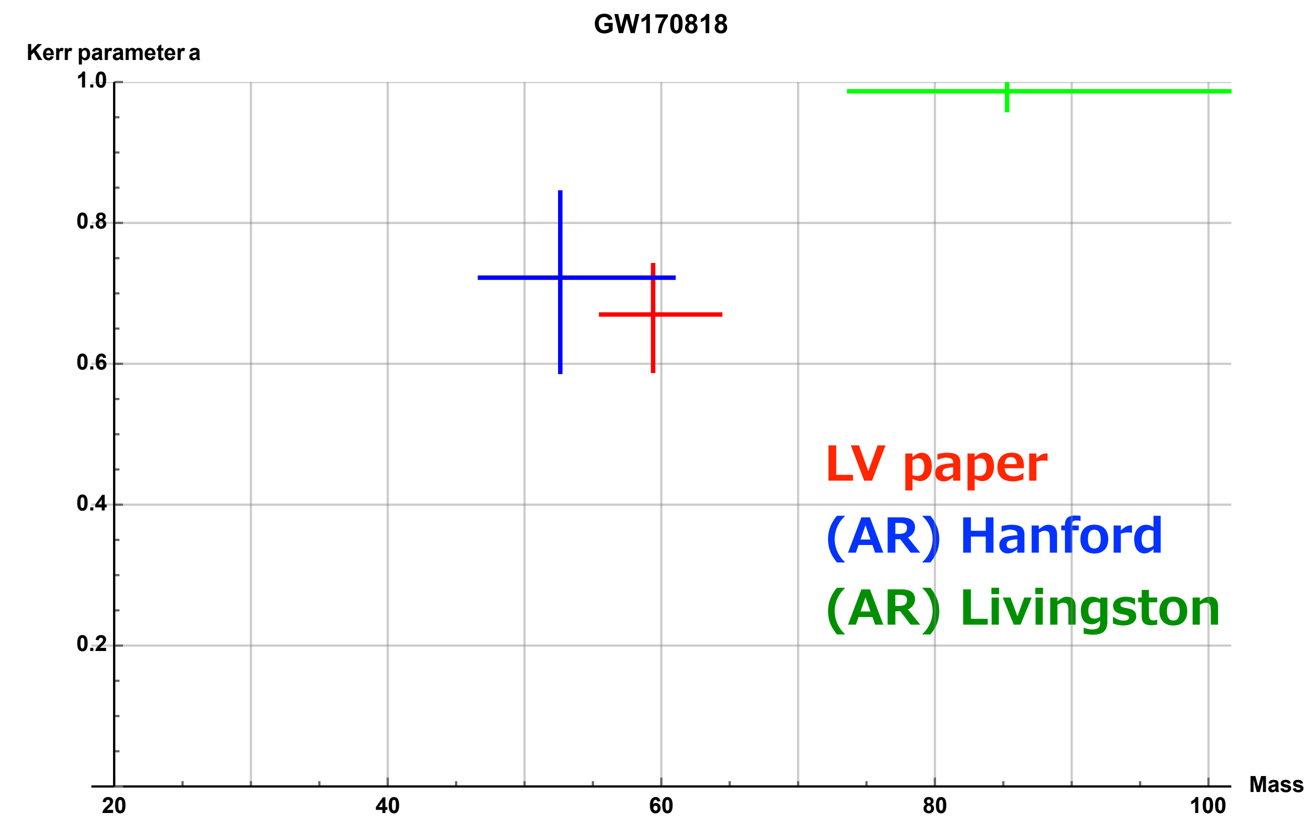

GW170823

LV paper ▶

$$(M, a) = (65.4^{+10.1}_{-7.4}, 0.72^{+0.09}_{-0.12})$$

f_{QNM} ▶

$f_{220} = 268.7$ Hz, $f_{221} = 263.5$ Hz, $f_{222} = 253.4$ Hz
$f_{210} = 364.4$ Hz, $f_{211} = 221.0$ Hz, $f_{200} = 243.1$ Hz
$f_{330} = 425.3$ Hz, $f_{331} = 422.2$ Hz, $f_{332} = 416.6$ Hz
$f_{320} = 380.1$ Hz, $f_{310} = 341.8$ Hz, $f_{300} = 310.1$ Hz

Hanford (SNR=6.8)

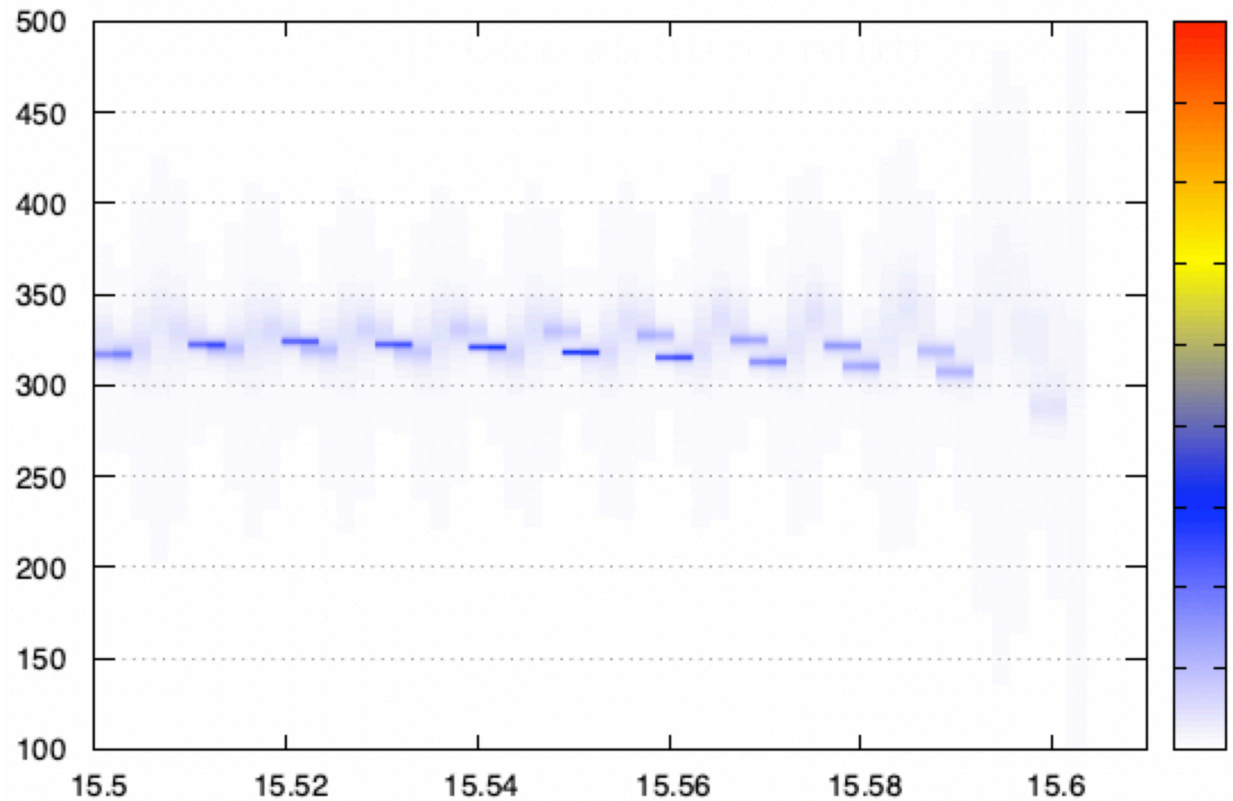

Livingston (SNR=9.2)

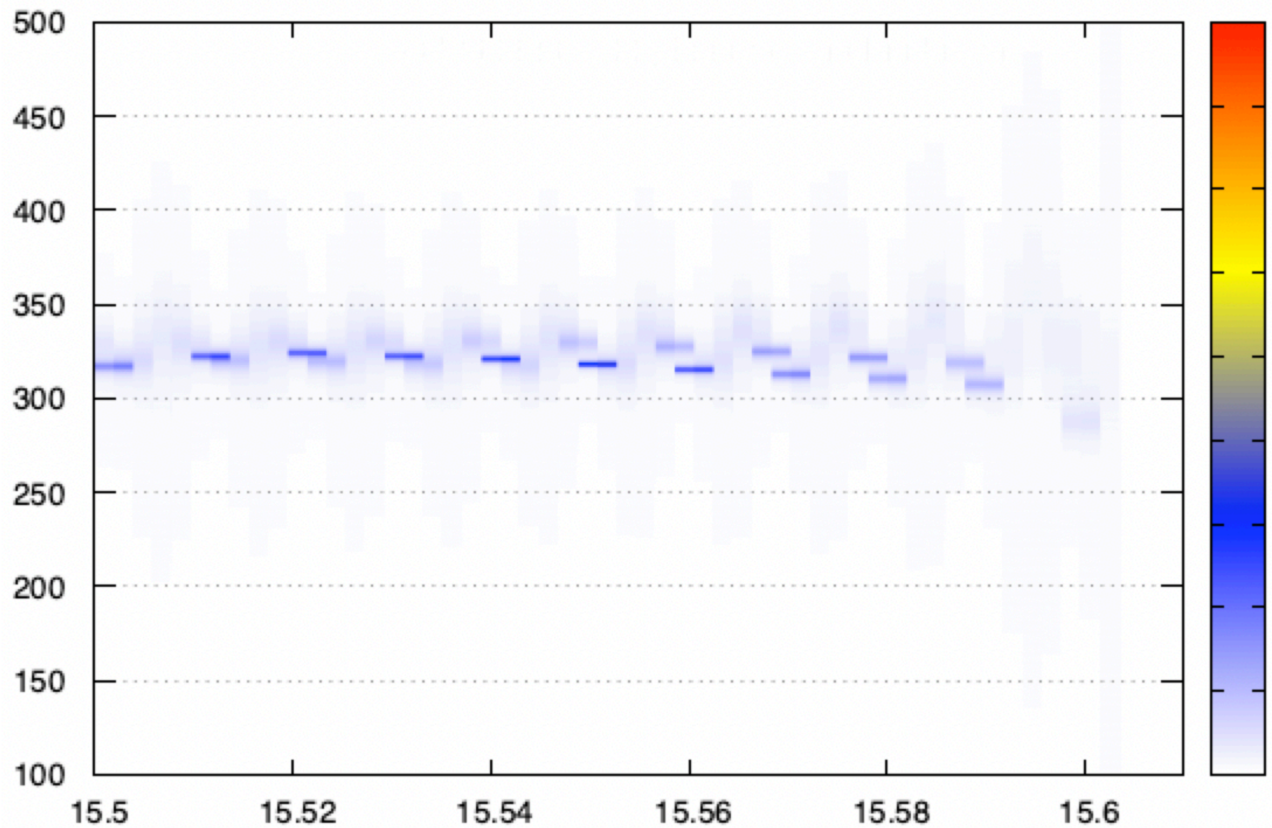

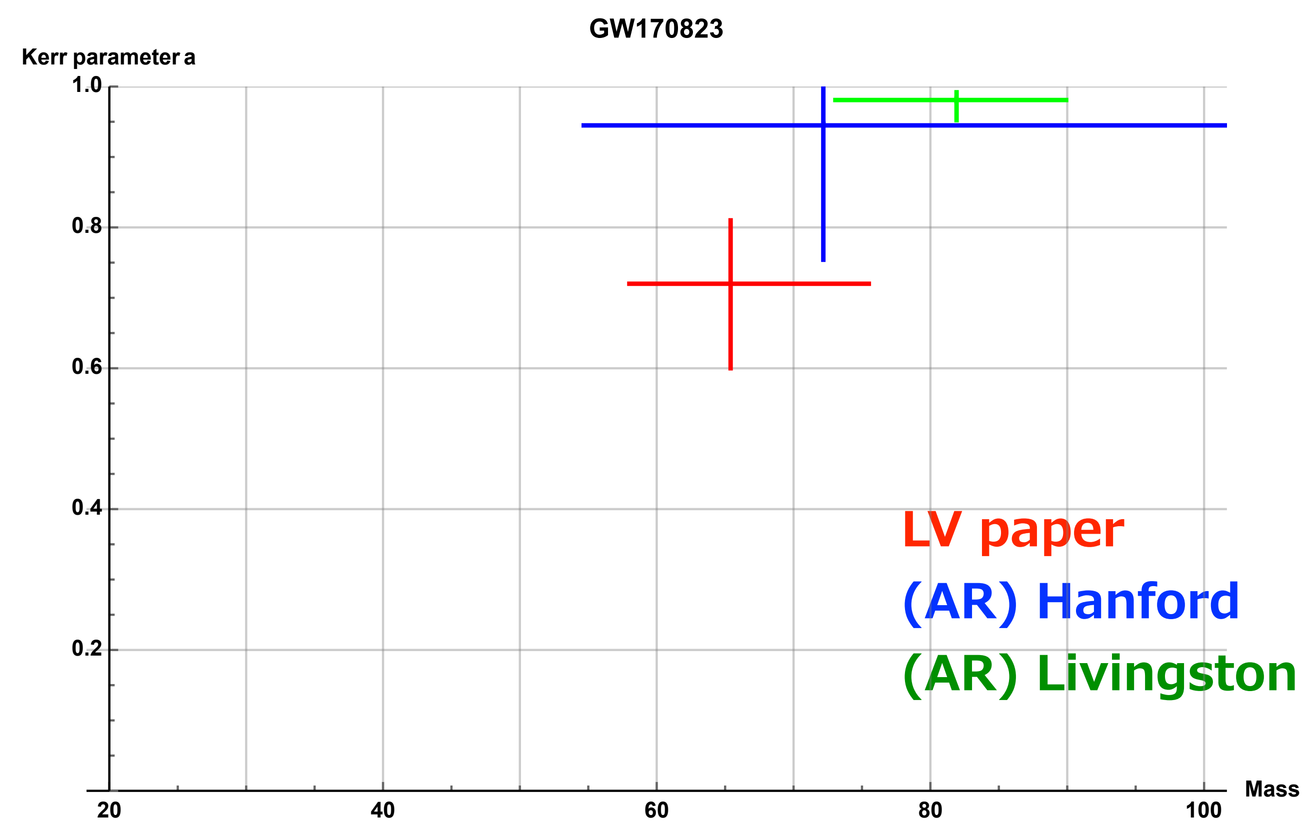

Summary & Outlook

自己回帰モデル *x(t)*

$$\begin{aligned} x_n &= a_1 x_{n-1} + a_2 x_{n-2} + \cdots + a_M x_{n-M} + \varepsilon \\ &= \sum_{j=1}^{M} a_j x_{n-j} + \varepsilon \end{aligned}$$

短いデータ (〜 60 pts) に対しても精度よく周波数・減衰率を特定できる.
シグナルを見つけるのにテンプレートは不要.

LIGO/Virgo の O1/O2イベントデータに適用，リングダウン部分の抽出を試みた.
SN比が高ければ，独立にリングダウン部分が取り出せそうだ.

★ノイズ除去の方法や，他の方法と組み合わせ，より精密な周波数特定法を開発中.
★higher modesの特定へ，BHの特長量の特定へ，相対論検証へ.
★テンプレートを使わない方法は，今後，未知の重力波シグナルの候補検出に役立つかも.